



RESEARCH ARTICLE

10.1029/2021MS002927

Comparing Model Representations of Physiological Limits on Transpiration at a Semi-Arid Ponderosa Pine Site

Linnia R. Hawkins¹ , Maoya Bassouni^{2,3}, William R. L. Anderegg⁴ , Martin D. Venturas⁵ , Stephen P. Good⁶ , Hyojung J. Kwon¹ , Chad V. Hanson¹, Richard P. Fiorella^{7,8} , Gabriel J. Bowen⁷ , and Christopher J. Still¹ 

¹Department of Forestry, Oregon State University, Corvallis, OR, USA, ²Department of Crop Production Ecology, Swedish University of Agricultural Sciences, Uppsala, Sweden, ³Department of Environmental Sciences, Policy, and Management, University of California, Berkeley, CA, USA, ⁴School of Biological Sciences, University of Utah, Salt Lake, UT, USA, ⁵Departamento de Sistemas y Recursos Naturales, Universidad Politécnica de Madrid, Madrid, Spain, ⁶Department of Biological and Ecological Engineering, Oregon State University, Corvallis, OR, USA, ⁷Department of Geology and Geophysics, University of Utah, Salt Lake, UT, USA, ⁸Earth and Environmental Sciences Division, Los Alamos National Laboratory, Los Alamos, NM, USA

Key Points:

- We evaluate several model formulations for coupling plant hydraulic and stomatal response using functional performance metrics
- Information flows from soil water potential and vapor pressure deficit to transpiration reflect structural differences among models
- Considerable biases in modeled canopy temperature propagate to a 5% offset in cumulative growing season transpiration

Supporting Information:

Supporting Information may be found in the online version of this article.

Correspondence to:

L. R. Hawkins,
Linnia.Hawkins@oregonstate.edu

Citation:

Hawkins, L. R., Bassouni, M., Anderegg, W. R. L., Venturas, M. D., Good, S. P., Kwon, H. J., et al. (2022). Comparing model representations of physiological limits on transpiration at a semi-arid ponderosa pine site. *Journal of Advances in Modeling Earth Systems*, 14, e2021MS002927. <https://doi.org/10.1029/2021MS002927>

Received 30 NOV 2021
Accepted 22 SEP 2022

Abstract Mechanistic representations of biogeochemical processes in ecosystem models are rapidly advancing, requiring advancements in model evaluation approaches. Here we quantify multiple aspects of model functional performance to evaluate improved process representations in ecosystem models. We compare semi-empirical stomatal models with hydraulic constraints against more mechanistic representations of stomatal and hydraulic functioning at a semi-arid pine site using a suite of metrics and analytical tools. We find that models generally perform similarly under unstressed conditions, but performance diverges under atmospheric and soil drought. The more empirical models better capture synergistic information flows between soil water potential and vapor pressure deficit to transpiration, while the more mechanistic models are overly deterministic. Although models can be parameterized to yield similar functional performance, alternate parameterizations could not overcome structural model constraints that underestimate the unique information contained in soil water potential about transpiration. Additionally, both multilayer canopy and big-leaf models were unable to capture the magnitude of canopy temperature divergence from air temperature, and we demonstrate that errors in leaf temperature can propagate to considerable error in simulated transpiration. This study demonstrates the value of merging underutilized observational data streams with emerging analytical tools to characterize ecosystem function and discriminate among model process representations.

Plain Language Summary Earth system models are an essential tool for understanding the consequences of changing climate conditions on forest ecosystems. Models are rapidly incorporating more realistic representations of how drought impacts ecosystem carbon and water cycling. These advancements need to be thoroughly evaluated to ensure that the models adequately capture the plant functional response to drought stress. Here we merge underutilized measurements with new analytical tools to evaluate several model representations of plant response to drought. These tools allow us to both better understand relationships among drought stress and ecosystem response, as well as quantify model accuracy. We find that models generally perform similarly under unstressed conditions, but performance diverges under drought.

1. Introduction

Climate change mitigation, adaptation, and conservation efforts all leverage ecosystem models to understand and predict carbon and water cycling at local to global scales. Ecosystem models have rapidly advanced in recent decades and now incorporate mechanistic representations of many plant and soil hydraulic processes (e.g., Eller et al., 2020; Kennedy et al., 2019; Sabot et al., 2020). Recent developments have focused on the representation of plant hydraulic functioning to improve mechanistic modeling of water transport through the soil-plant-atmosphere (SPA) continuum, but how best to represent the effects of drought stress on plant gas-exchange, especially when quantifying ecosystem-scale fluxes, is still an open question (Mencuccini et al., 2019). Evaluating improved plant hydraulic representation in ecosystem models requires more comprehensive frameworks for quantifying model performance, including both metrics for evaluating functional relations among processes, and comparisons against underutilized observational data.

© 2022 The Authors. Journal of Advances in Modeling Earth Systems published by Wiley Periodicals LLC on behalf of American Geophysical Union. This is an open access article under the terms of the [Creative Commons Attribution-NonCommercial License](https://creativecommons.org/licenses/by/4.0/), which permits use, distribution and reproduction in any medium, provided the original work is properly cited and is not used for commercial purposes.

Early land surface models (e.g., Bonan, 1995; Cox et al., 1998) implemented an empirical model for stomatal functioning based on gas-exchange measurements (Ball et al., 1987), which has been used for decades with strong empirical support (e.g., Damour et al., 2010; Lin et al., 2015). However, an ecological theory of stomatal functioning (Cowan & Farquhar, 1977) assumes plants optimize stomatal behavior such that the benefit of carbon gained (A) is equivalent to the respective cost of water loss by way of transpiration (T). As such, stomata optimize the tradeoff between carbon gain and the carbon cost of transpiration, $A - \lambda T$, where λ (mol CO₂/mol H₂O) is the carbon cost per unit water used by the plant. This theoretical basis has been used to develop semi-empirical stomatal models (Medlyn et al., 2011), which have been shown to be consistent with the same physiological principles as the Ball et al. (1987) model (Franks et al., 2017). Semi-empirical models are limited by the need to prescribe a constant value for λ , which does not respond to environmental conditions and is not based on measurable plant traits (Buckley, 2017). Optimization theory supports the conceptual framework of hydraulic limitation on gas exchange since the cost of hydraulic damage can be incorporated into the cost of water loss. Although there is still much discussion about how hydraulic functioning should be applied in semi-empirical models (Lin et al., 2015), hydraulic limitations have been incorporated into semi-empirical stomatal models (Kennedy et al., 2019; Sabot et al., 2022; Tuzet et al., 2003; Wolf et al., 2016; Xu et al., 2016; Yang et al., 2019; Zhou et al., 2013).

To directly couple stomatal conductance to plant hydraulic mechanisms, model formulations of optimal stomatal behavior have been proposed that assume plants balance carbon gain against hydraulic risk (e.g., Mencuccini et al., 2019; Sperry et al., 2017; Wang et al., 2020; Williams et al., 1996). The mechanistic optimization models have the advantage of being parameterized with measurable plant traits (although some parameters are still fit during calibration) and have been shown to perform well at the plant scale (e.g., Venturas et al., 2018; Wang et al., 2020). A comparison of different stomatal optimization principles in a big-leaf framework, indicated that formulations with explicit representation of plant hydraulics did not substantially improve ecosystem-scale evapotranspiration estimates (Bassiouni & Vico, 2021). At the ecosystem scale, Sabot et al. (2020) found that the Sperry et al. (2017) model demonstrated improved performance over the Medlyn et al. (2011) model and Bonan et al. (2014) showed that the SPA optimization model (Williams et al., 1996) demonstrated some improvement over the Ball et al. (1987) model when water availability was limited. However, both evaluations only compared the more mechanistic models against semi-empirical models without hydraulic constraints. Sabot et al. (2022) compared several empirical formulations with soil moisture stress functions against optimization approaches embedded in a land surface model. They found that the Sperry et al. (2017) optimization model outperformed the Medlyn et al. (2011) model even with a soil moisture stress function, and that good performance can result from misrepresentation of physiological processes.

Here we compare semi-empirical models with hydraulic constraints against more mechanistic optimization models at the ecosystem scale. We implement hydraulic constraints within the Ball et al. (1987) and Medlyn et al. (2011) models by altering the water use efficiency parameter as a function of the leaf water potential. We evaluate these hydraulic-modified semi-empirical models against two mechanistic approaches. One approach was developed by Williams et al. (1996) in the SPA model where the stomatal conductance is calculated to optimize water-use efficiency while avoiding hydraulic failure. This model conceptualizes hydraulic failure by a simple minimum leaf water potential threshold. Another approach we evaluate here is the Sperry et al. (2017) model of optimal stomatal behavior which assumes plants maximize carbon gain while avoiding hydraulic risk. This model integrates across xylem elements to determine the hydraulic vulnerability at an instantaneous drop in canopy water potential.

Model inter-comparisons are commonly performed by benchmarking the mean state and variability of simulated carbon and water fluxes against observations (e.g., Kennedy et al., 2019; Sabot et al., 2020). But it is particularly important to ensure that the functional relationships among environmental conditions and ecosystem responses are also adequately captured (Bassiouni & Vico, 2021; Goodwell & Bassiouni, 2022; Ruddell et al., 2019; Sabot et al., 2022), particularly when models are intended to make future projections. We leverage ecosystem-scale measurements from a long running intensively monitored AmeriFlux core site equipped with sap-flux instrumentation in a seasonally drought stressed ecosystem and employ a suite of functional performance diagnostics designed to disentangle physiological limits on transpiration. We evaluate the influence of different model process representations on the simulated functional relationships among meteorological conditions, soil water availability, and transpiration at diurnal to monthly time scales and for a range of atmospheric and/or soil water

Table 1
Canopy Structure, Root Distribution and Photosynthesis Parameter Values Used in Models

Model	Description	Units	Value	Source
All	Leaf area index	$\text{m}^2 \text{m}^{-2}$	2.8	Irvine et al. (2004)
All	Leaf carbon per leaf area	gC m^{-2} leaf area	122.4	Ruehr et al. (2014)
All	Maximum rooting depth	m	1.1	Ruehr et al. (2014)
All	Total root biomass	g m^{-2}	70	Ruehr et al. (2014)
All	V _{max} at 25°C	$\mu\text{mol m}^{-2} \text{s}^{-1}$	31.4	Ruehr et al. (2014)
All	J _{max} at 25°C	$\mu\text{mol m}^{-2} \text{s}^{-1}$	52.4	Ruehr et al. (2014)
All	Canopy height	m	18	Ruehr et al. (2014)
SPA	Height of canopy layers	m	18,15.9,15.1,14.2,13.3,11.8,9	Defined to have equal LAI and follow canopy structure.
SPA	Average foliar nitrogen	gN m^{-2} leaf area	2.1	Schwarz et al. (2004)
SPA	Plant capacitance	$\text{mmol H}_2\text{O m}^{-2}$ leaf area MPa^{-1}	2,500	Bonan et al. (2014)
SPA	Root resistivity	MPa s g mmol^{-1}	20	Ruehr et al. (2014)
Gain-Risk	Leaf area:basal area	$\text{m}^2 \text{m}^{-2}$	878	Irvine et al. (2004)
Gain-Risk	Basal area:ground area	$\text{m}^2 \text{Ha}^{-1}$	31.9	Irvine et al. (2004)
Gain-Risk	Rhizosphere resistivity	(%)	50	Venturas et al. (2018)

stressed conditions. This study demonstrates the value of merging observational data and emerging analytical tools to characterize ecosystem function and discriminate among model representations.

2. Methods

2.1. Site and Observational Data Description

The Metolius forest study site is in a mature coniferous forest in central Oregon at an elevation of 1,253 m asl. The forest is a core research site in the AmeriFlux network (site US-Me2) where microclimate and eddy-covariance flux measurements are collected from a flux tower. The canopy is dominated by ponderosa pine trees (*Pinus ponderosa*) with scattered incense cedars (*Calocedrus decurrens*). Trees are evenly distributed with a leaf area index (LAI) of 2.8 (m^2 leaf m^{-2} ground). Tree height is relatively homogeneous at about 18 m, and the mean tree density is approximately 339 trees ha^{-1} (Irvine et al., 2008). The climate is semi-arid, with warm and dry summers and cool and wet winters, with most precipitation occurring as snow or rain during the winter and spring (November through April). Additional descriptions of the study site, as well as information on site instrumentation and measurements, can be found in Law et al. (2001), Irvine et al. (2004), Thomas et al. (2009) and Ruehr et al. (2014). In this study, we examine the period of 1 January 2006 to 31 December 2018 where the observational records of data streams overlap. We define the growing season as 1 May to 31 August which coincides with the warmest and driest months of the year at this site.

The US-Me2 site is instrumented with a 33 m tower measuring above canopy eddy-covariance fluxes of CO_2 , H_2O , latent and sensible heat. Mature ponderosas have been instrumented with sapflow probes which are used to estimate whole tree transpiration by scaling with estimates of sapwood area (see Kwon et al., 2018). We also calculate the canopy conductance per unit ground area (G_c , mm/s) from the sapflow estimates of transpiration, air temperature (T_a , °C), and vapor pressure deficit (VPD, kPa) using a simplified form of the Penman-Monteith equation as suggested by Monteith and Unsworth (1990) as is typically used in ecohydrological studies (Kwon et al., 2018). Canopy temperature was also measured in 2015 (Kim et al., 2016) using a thermal camera (FLIR A325sc). The thermal camera measured the temperature of the upper canopy and we averaged over a selected area of interest to represent only canopy foliage. Soil probes measure soil water content at 10, 20, 30, 50, 70, 100, 130, and 160 cm depths (Sentek Technologies, Stepney, SA, Australia). We calculated the root weighted soil water potential using the relationship between soil water content and water retention from Ruehr et al. (2014) and the root profile prescribed in the SPA model (Table 1).

2.2. SPA Multi-Layer Canopy Model Description

The Soil-Plant-Atmosphere model (SPA; Williams et al., 1996, 2001a) is a high vertical resolution point model (up to 10 canopy layers and 20 soil layers) which simulates exchanges of carbon, water, and energy between the land surface and atmosphere on 30-minute timesteps. The SPA model has been used for a variety of applications including site level analyses of carbon and water fluxes (Ruehr et al., 2014; Williams et al., 1996; Williams, Law, et al., 2001a, Williams, Rastetter, et al., 2001b); model intercomparisons of stomatal and hydraulic functioning (Bonan et al., 2014; Misson et al., 2004); data assimilation (Sus et al., 2014; Williams et al., 2005); and modeling land-atmosphere feedbacks (Hill et al., 2008; Smallman et al., 2013). In this study, we implemented several model updates including those from a recent study which used the SPA model to simulate the carbon cycle at US-Me2 under current and future climate conditions (Ruehr et al., 2014).

The SPA model includes a detailed radiative transfer scheme for long-wave, near infra-red, and direct and diffuse photosynthetically active radiation to determine transmittance, reflectance, and absorption in each canopy layer for sunlit and shaded leaf fractions. The SPA model assumes within-canopy air is well-mixed and thus does not resolve the vertical profile of air temperature, or CO₂ but the leaf energy balance is calculated for each layer independently. Leaf energy balance is coupled to a widely used biochemical model of photosynthesis (Farquhar and von Caemmerer, 1982) and leaf transpiration through an optimization scheme for stomatal conductance. In this study's implementation, rather than using the Penman-Monteith equation for leaf transpiration, we calculated transpiration directly from Fick's law as:

$$T = \frac{g_w * D_l}{P_a} \quad (1)$$

where T is the transpiration rate per unit leaf area (mmol m⁻² s⁻¹), g_w is the two-sided leaf total conductance (series of stomatal and leaf boundary layer) to water vapor (mmol m⁻² s⁻¹), P_a is the atmospheric pressure (kPa) and D_l is the leaf-specific vapor deficit (kPa) calculated as a function of leaf temperature (T_{leaf}):

$$D_l = e_s(T_{\text{leaf}}) - \frac{e_s(T_{\text{air}}) * h}{100} \quad (2)$$

Where $e_s(T_{\text{leaf}})$ is the saturation vapor pressure at leaf temperature and $e_s(T_{\text{air}})$ is the saturation vapor pressure at the air temperature and h is the relative humidity (%) (Grossiord et al., 2020).

The SPA model calculates stomatal conductance for each canopy layer based on a hypothesis that stomatal conductance is regulated to prevent hydraulic failure (Williams et al., 1996, Williams, Law, et al., 2001a). The transport of water through the soil-plant-atmosphere continuum flows down a potential gradient at a rate proportional to the whole-plant conductance. The plant conductance is a static function of hydraulic architecture, xylem construction, and leaf conductance and the soil-to-root conductance is a function of soil hydraulic conductivity and root density. Following Ruehr et al. (2014), we reduced whole plant conductance in response to declining soil water potential according to a sigmoid function and reduced the soil tortuosity and soil surface roughness length to increase soil water evaporation and better match observations.

In this application, we used six canopy layers, each with equivalent LAI but varied thickness to approximate canopy structure (Reinhardt et al., 2006). The vertical soil profile was defined by 20 soil layers of 0.1 m thickness with soil texture defined as in Law et al. (2001). We modified the SPA model to run using prescribed soil water content in an effort to remove feedbacks between transpiration and soil moisture. For example, models that simulate lower transpiration in spring may retain soil moisture through the dry season thus relaxing drought stress which introduces a confounding factor into the model inter-comparison. Furthermore, we implemented a site-specific empirical relationship between soil water content and soil water potential following Ruehr et al. (2014). This modification ensured the matric potential of the soil is identical across models, isolating the differences in water stress across models to the representation of plant hydraulics rather than soil water retention functions. However, this decision also removes important feedbacks between transpiration and soil water potential that do occur and are important influences on stomatal response across time scales. At the US-Me2 site, the loss of water from the land surface to the atmosphere through evapotranspiration exceeds the total input of precipitation in some years. This phenomenon cannot be represented by process models without ground water pools which is another motivation for prescribing soil water content. Configuration of canopy structure, photosynthesis

parameters, and rooting profile can be found in Table 1, and we provide more information on model updates in Supporting Information S1.

2.3. Stomatal Sub-Models in SPA

We compared four sub-models with unique assumptions regarding stomatal behavior within the SPA model framework, each including explicit hydraulic mechanisms that down regulate stomatal conductance in response to more negative plant water potential. We implemented hydraulic constraints to the Ball et al. (1987) model (hereafter referred to as BB-H) and the Medlyn et al. (2011) model (MED-H); and use two different definitions of stomatal efficiency in the SPA optimization scheme based on intrinsic water use efficiency ($WUE_i, A/g_w$) and the ratio of CO_2 assimilation to transpiration ($WUE, A/T$).

The predominant semi-empirical model for stomatal functioning was developed by Ball et al. (1987) who defined a simple linear approximation of the relationship between photosynthesis and stomatal conductance to water (g_w ; $mol\ H_2O\ m^{-2}\ s^{-1}$) based on gas exchange data:

$$g_w = g_0 + g_{1B} \left(\frac{A * h}{C_a} \right) \quad (3)$$

where A is the net assimilation rate ($\mu mol\ CO_2\ m^{-2}\ s^{-1}$), h is the relative humidity at the leaf surface ($mol\ mol^{-1}$), C_a is the atmospheric CO_2 concentration at the leaf surface ($\mu mol\ mol^{-1}$) and g_0 and g_{1B} are fitted parameters. While g_0 and g_{1B} are determined by fitting the equation to leaf-gas exchange data, both represent physiologically meaningful quantities (Franks et al., 2017). The intercept parameter, g_0 , is the minimum stomatal conductance and is usually close to zero. We set g_0 to 0.1 as in Franks et al. (2017) throughout this study. The slope parameter, g_{1B} , is generally representative of g_w/A , the reciprocal of the intrinsic water use efficiency, A/g_w (Farquhar, 1989; Feng, 1999). The Ball et al. (1987) model assumes that stomata respond to relative humidity at the leaf level, but it is more likely that stomata sense water fluxes (Aphalo & Jarvis, 1991) and respond to changes in water status of the leaf tissue (Buckley, 2005, 2019).

An alternative framework for stomatal function was developed by Cowan and Farquhar (1977) based on the premise that optimal stomatal behavior maximizes carbon gain minus the carbon cost of water loss, $A - \lambda T$, where λ is often defined as the water use efficiency. By combining theory of optimal stomatal control (Cowan & Farquhar, 1977) and photosynthesis (Farquhar et al., 1980), Medlyn et al. (2011) derived the following expression for stomatal conductance:

$$g_w = g_0 + 1.6 \left(1 + \frac{g_{1M}}{\sqrt{VPD}} \right) \frac{A}{C_a} \quad (4)$$

Where VPD is the vapor pressure deficit (kPa), and g_0 and g_{1M} are fit parameters. Despite having a similar form to the Ball et al. (1987) model, the fit parameter g_{1M} in the Medlyn et al. (2011) model has a different theoretical interpretation: g_{1M} is proportional to the marginal water cost of carbon (λ) and the CO_2 compensation point (Γ^*):

$$g_{1M} = \sqrt{\frac{3\Gamma^* \lambda}{1.6}} \quad (5)$$

In this application, we introduce a hydraulic constraint into the Ball et al. (1987) and Medlyn et al. (2011) stomatal models similarly to the approach of Wolf et al. (2016). At short time scales, λ is usually treated as an unknown fitted constant but λ can also be determined from system boundary conditions and generally follows an exponential function with soil moisture (Cowan, 1986; Mäkelä et al., 1996; Manzoni et al., 2013), therefore supporting our semi-empirical model variations. Specifically, the instantaneous leaf water potential in each canopy layer modifies the g_1 parameter (g_{1B} or g_{1M}) according to a Weibull function based on the leaf hydraulic vulnerability curve as:

$$g_1 = g_{10} * e^{-\left(\frac{-\psi_l}{b}\right)^c} \quad (6)$$

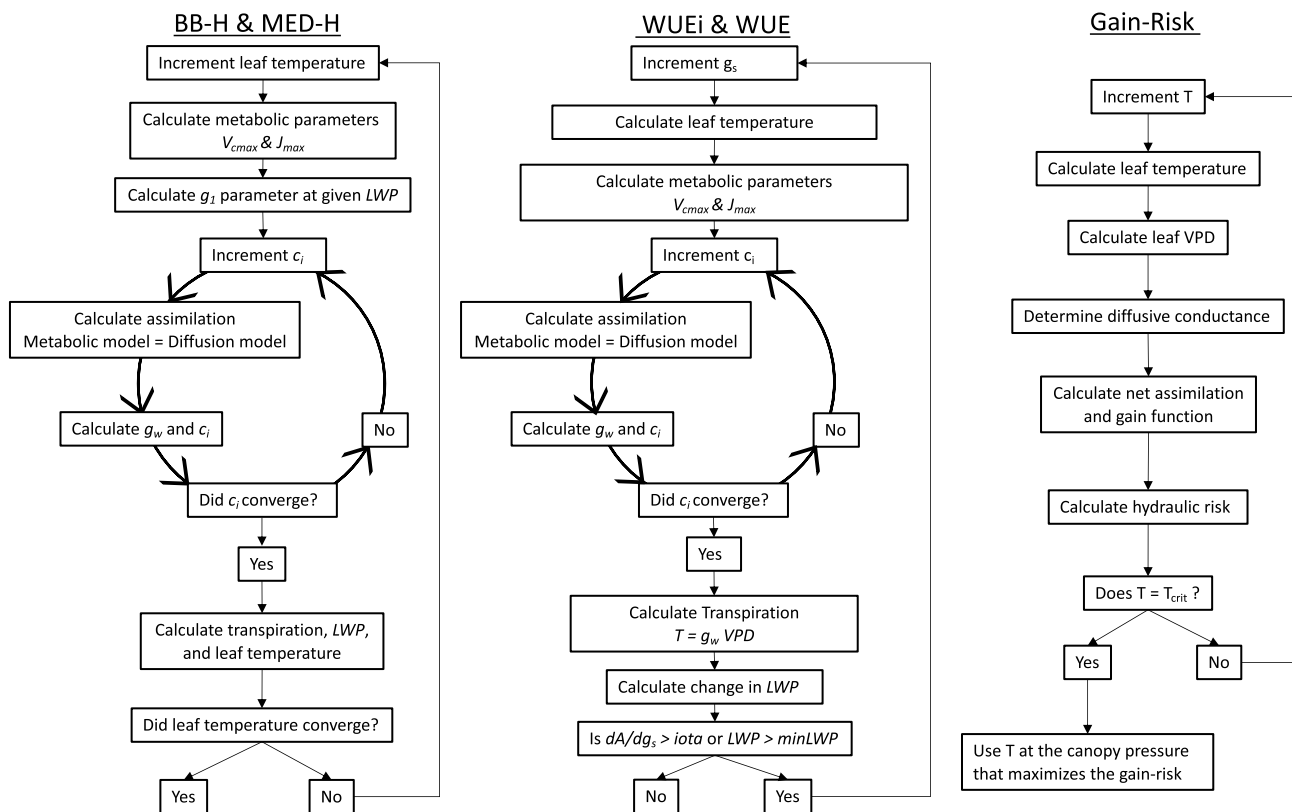


Figure 1. Schematic of leaf flux calculations using the BB-H and MED-H models in the soil-plant-atmosphere (SPA) model (left), the intrinsic water use efficiency (WUEi) and WUE optimizations in the SPA model (center), and the Gain-Risk model (right).

Where g_{10} is the value of g_1 when soil water potential is near zero, ψ_l represents the instantaneous leaf water potential (MPa), and the Weibull b and c parameters are fitted according to measurements of ponderosa pine leaf hydraulic vulnerability (Figure S1 in Supporting Information S1). Hereafter we refer to the Ball et al. (1987) and Medlyn et al. (2011) models with hydraulic constraints as BB-H and MED-H, respectively.

In the default SPA model, stomatal conductance shares some commonalities with theory of optimal stomatal behavior (Cowan & Farquhar, 1977). Stomatal conductance is calculated to maximize assimilation, given transport of water from soil-to-leaf, plant water storage, and hydraulic safety margins (Figure 1). The optimization scheme incrementally increases stomatal aperture until further opening either: (a) does not increase carbon gain per unit water loss (defined by the stomatal efficiency parameter); or (b) causes leaf water potential to drop below a pre-set minimum value (minLWP). The stomatal efficiency is defined as the assimilation divided by the stomatal conductance to water (A/g_w) and we refer to this version of the SPA model as WUEi. Bonan et al. (2014) introduced an alternate definition of stomatal efficiency into the SPA model, A/T , which we refer to as WUE. Both implementations can represent conservative to more intensive plant water use behavior. For example, conservative behavior is achieved by setting a higher stomatal efficiency value and increasing the amount of appreciable carbon gain per unit increase in stomatal opening. As a result, excessive transpiration is avoided in the morning when atmospheric demand is low in order to preserve water to buffer the effects of high mid-day atmospheric demands (i.e., more isohydric behavior). Low values of stomatal efficiency result in intensive water use (higher optimal g_w and more transpiration).

2.4. Gain-Risk Big-Leaf Model Description

We also applied the model of Sperry et al. (2017), a big-leaf model with five soil layers (hereafter referred to as the Gain-Risk model). Stomatal functioning in the Gain-Risk model is based on optimization theory and assumes plants maximize carbon gain while minimizing hydraulic risk (Anderegg et al., 2018; Sperry & Love, 2015; Sperry et al., 2016, 2017; Venturas et al., 2021; Wolf et al., 2016). The resulting coordination between stomatal

and xylem functioning agrees well with observations (Meinzer et al., 2009) and more strongly agrees with leaf-level gas exchange data than the classic Cowan-Farquhar based optimization models (Anderegg et al., 2018; Wang et al., 2020). Carbon gain is calculated as in the SPA model (Farquhar et al., 1980) and the carbon gain function, α , is defined at a given value of T as:

$$\alpha = \frac{A_{\text{net}}}{A_{\text{max}}} \quad (7)$$

Hydraulic risk is defined as the fractional loss of hydraulic conductance. Vulnerability to cavitation curves (VC's) for each xylem element (roots, stem, and leaves) are represented by two-parameter Weibull functions:

$$K(P_x) = K_{\text{max}} * e^{-\left(\frac{-P_x}{b}\right)^c} \quad (8)$$

Where K is the hydraulic conductance, K_{max} is the maximum hydraulic conductance, P_x is the pressure imposed on each xylem element, and b and c are fit parameters (Figure S1 in Supporting Information S1). At each increment in T , the pressure drop across xylem elements ($P_{x(\text{up})} - P_{x(\text{down})}$) is calculated and the supply function is then defined as the relationship between T and P_x :

$$T = \int_{P_{x(\text{up})}}^{P_{x(\text{down})}} K(P_x) dp \quad (9)$$

The hydraulic risk function (θ) is defined as the fractional loss in canopy hydraulic conductance (K_c) at a given value of T :

$$\theta = 1 - \frac{K_c(P_c)}{K_{c\text{max}}} \quad (10)$$

Where P_c is the canopy water potential, and $K_{c\text{max}}$ is the maximum hydraulic conductance of the canopy. The Gain-Risk model finds the optimal stomatal conductance by incrementing T from zero and calculating the marginal carbon gain α , given the environmental conditions at that time step. The hydraulic risk is calculated from the change in canopy water potential, P_c , and the optimal T rate is that which maximizes the difference between the carbon gain function and the hydraulic risk function; $\max(\alpha - \theta)$. The stomatal conductance is then calculated from the optimal T and the VPD at that time step as in the SPA model. Fluxes are then scaled from leaf area to basal area to ground area using measurements from Irvine et al. (2004) (Table 1). We ran the Gain-Risk model without xylem refilling to capture permanent losses in hydraulic conductivity that lead to reductions in transpiration and assimilation after a drought. To ensure that soil water stress was identical across models we prescribed soil water potential in the Gain-Risk model from measurements of soil water content and measured soil water retention curves as with the SPA model.

2.5. Parameterization of Stomatal Sub-Models and Hydraulic Function

We prescribed model parameter values based on plant trait measurements available in the literature rather than best-fit calibrations in order to reflect how formulations may be used in Earth System Models. Additionally, our goal was to ensure that all parameters with the same mechanistic meaning were equivalent. Therefore, differences in model performances better reflect adequacy of model structures versus differences due to varying parameter calibrations.

Franks et al. (2017) demonstrated that equivalent g_1 parameter values for the Ball et al. (1987) and Medlyn et al. (2011) models can be derived as:

$$g_{1B} \approx \frac{1.6}{h} * \left(1 + \frac{g_{1M}}{\sqrt{\text{VPD}}}\right) \quad (11)$$

Additionally, the WUE stomatal efficiency parameter ($iota$) in the SPA model is equivalent to $1/\lambda$ thus Equations 4 and 5 can be used to determine the equivalent value of $iota$ for a given value of the g_{1M} parameter. In this application we set the Medlyn et al. (2011) g_{1M} parameter to 2.35, determined from gas-exchange data in Lin

Table 2
Stomatal Conductance Model Parameter Definitions, Values, and Perturbation Ranges for Sensitivity Analysis

BB-H	Parameter	Unit	Value	Range
g_{1B}	Fit parameter	Unitless	14.2	(6, 14)
Weibull b	VC parameter	-MPa	2.8	(1, 5)
Weibull c	VC parameter	Unitless	3.7	(1, 5)
MED-H				
g_{1M}	Fit parameter	kPa ^{0.5}	2.35	(1, 5)
Weibull b	VC parameter	-MPa	2.8	(1, 5)
Weibull c	VC parameter	unitless	3.7	(1, 5)
WUEi/WUE				
g_{plant}	Leaf specific conductance	Mmol m ⁻² s ⁻¹ MPa ⁻¹	8.2	(3, 30)
$minLWP$	Minimum leaf water potential	MPa	-2	(-5, -1.7)
$iota$	Stomatal efficiency (WUEi: dA/dg _s , WUE: dA/dE)	(umol CO ₂ /molH ₂ O)	0.0135/1,350	(0.00375,0.03) (375, 3,000)
Gain-risk				
K_{max}	Maximum conductivity	kg h ⁻¹ MPa ⁻¹ m ⁻²	120	(43, 424)
LSC	Leaf specific conductance	Mmol m ⁻² s ⁻¹ MPa ⁻¹	8.2	(3, 30)
Weibull b	VC parameter	-MPa (root/stem/leaf)	1.56/4/2.8	(0.8, 2.2)
Weibull c	VC parameter	unitless (root/stem/leaf)	1.4/3.4/3.7	(2, 3.5)

et al. (2015) representing needleleaf plant functional types. We determined g_{1B} and $iota$ from Equations 11 and 5, respectively, with air temperature = 25°C, $h = 0.45$, and $\Gamma^* = 40 \mu\text{mol/mol}$ (Table 2). The Gain-Risk model does not have an equivalent parameter since the water use efficiency is diagnosed from the relationship between carbon gain and hydraulic risk.

The Gain-Risk, WUEi and WUE models all use the leaf specific conductance, which was set to 8.2 mmol m⁻² s⁻¹ MPa⁻¹ for a Ponderosa pine as per Johnson et al. (2009). The leaf and root hydraulic vulnerability curves used in the Gain-Risk model were from previous studies of ponderosa pine (Sperry et al., 2019), while the stem VC was measured at the site but agrees well with literature values used by Sperry et al. (2019). Although the BB-H and MED-H approaches impose hydraulic limitation on stomatal functioning differently than the Gain-Risk model, we used consistent Weibull b and c parameters from the leaf VC in Equation 7 (Figure S1 in Supporting Information S1).

In this study we always assumed plants modify stomatal function instantaneously. The original formulations of WUEi, WUE, and Gain-Risk models modify the water use efficiency in response to hydraulic constraints on instantaneous timescales. For consistency, we made the same assumption in the BB-H and MED-H models by modifying the g_1 parameter based on instantaneous ψ_l . Though there is insufficient observational evidence to indicate whether stomata respond instantaneously to stimuli, we tested our assumption by comparing simulated canopy conductance using the predawn versus instantaneous ψ_l to represent slower versus faster responses of water use efficiency to hydraulic stress. We found that the simulated canopy conductance better matched the diurnal shape of the observed canopy conductance when the instantaneous ψ_l was used (Figure S2 in Supporting Information S1). Continuous measurements of canopy water potential are needed to help constrain these processes and inform model representation. Additionally, all models used in this study assumed hydraulic stress only modified stomatal function, but there is ongoing debate on how non-stomatal responses to hydraulic stress should be implemented in ecosystem models (Zhou et al., 2013).

2.6. Model Performance Evaluation

We defined a series of diagnostics to quantify and compare model functional performance under conditions spanning well-watered conditions to atmospheric and/or soil drought stressed conditions. We employed three evaluation strategies, including the analysis of (a) diurnal processes individually; (b) effective functional relations

between processes and an environmental driver; (c) joint causal relations and functional performance metrics based on information theory. We grouped the data (May–August of 2006–2018) according to inter-quartile ranges of SWP and VPD to examine varying degrees to atmospheric and/or soil water stress. We aggregated SPA leaf-level process simulations over all canopy layers, scaled by the assimilation in the sunlit and shaded fraction of each layer to compare to the ecosystem-scale observations and to maintain consistency with the Gain-Risk model that takes a big-leaf approach (with sunlit and shaded fractions).

2.6.1. Diurnal Processes

We first explored modeled ecosystem-scale processes on diurnal time scales to understand how model assumptions manifest. We compared models in terms of diurnal simulations of transpiration (T); canopy conductance (G_c); canopy water potential (P); gross primary production (GPP); the ratio of internal to external partial pressure of CO_2 (C_i/C_a); and the difference between canopy and air temperature ($T_{\text{can}} - T_{\text{air}}$). We then compared the simulated diurnal cycle of T under four different levels of atmospheric and/or soil water drought stress to examine how model assumptions affect the diurnal cycle of T in response to environmental stress. We also focused on differences between observed and modeled T_{can} because it plays a critical role in the calculation of photosynthetic rates and in the optimization of stomatal conductance. T_{can} can diverge from the T_{air} by several degrees, particularly when T_{air} is high (Kim et al., 2016) which can have large consequences for leaf metabolic processes (Still et al., 2019). To illustrate the consequences of T_{can} biases we performed simulations with the MED-H model where we prescribed model leaf temperature as the measured T_{can} .

2.6.2. Response to Environmental Drivers

We then evaluated how different model representations influence the sensitivity of G_c to VPD under both low and high soil water stress following Novick et al. (2016). We derived G_c empirically from sapflow and meteorological data and scaled the empirical and modeled G_c estimates by their respective seasonal maximum. We fit an exponential decay function to the rescaled data and compared G_c sensitivity to VPD in observations and models during low water stress days (SWP >75th percentile) high water stress days (SWP <25th percentile) separately. We quantified uncertainty in the empirical pattern by modifying the sapflow-derived transpiration by $\pm 40\%$ and re-calculating G_c .

We also examined differences in model relations between water use efficiency and water potential. Water use efficiency was defined here as assimilation divided by transpiration (A/T) and assessed on monthly time scales. Another measure of water use efficiency is the ratio C_i/C_a which is thought to be a balance point between the stomatal supply and photosynthetic demand for CO_2 . C_i/C_a can be inferred from observed ratios of ^{13}C – ^{12}C in cellulose in leaf tissue or tree rings ($\Delta^{13}\text{C}$), which have been previously used to constrain model uncertainties (Lavergne et al., 2019). Although observations of $\Delta^{13}\text{C}$ were not available at this site, comparing C_i/C_a across models is a useful exercise for illustrating the modeled water-use strategies.

2.6.3. Joint Causal Relations Based on Information Theory

We used functional accuracy metrics based on information theory to quantify the ability of models to reproduce the daily causal influence of atmospheric water demand and soil water supply together on T as a mapping of inputs to outputs. We therefore used non-parametric information partitioning metrics to evaluate how models represent hydraulic function and feedbacks on gas exchange overall, which are especially relevant because ecosystem-scale data and processes are highly uncertain (Bassiouni & Vico, 2021) and are driven by correlated variables (Goodwell & Bassiouni, 2022). Information theory is based on Shannon Entropy (Shannon, 1948), a measure of uncertainty in a random variable or the information required to fully predict that variable. Mutual information is a measure of the reduction of uncertainty or shared information that knowledge of another variable can provide (Cover & Thomas, 2012). Quantifying this shared information among environmental variables, or information flows, has been proven useful in inferring causal interactions among variables in complex ecohydrological systems (Goodwell et al., 2020; Ruddell & Kumar, 2009) and in diagnosing how information flows through ecohydrological models (Li & Good, 2021).

Specifically, we quantified the information VPD and SWP together provide about observed and modeled T . This quantity, the multivariate mutual information, can be partitioned into four non-negative components (Goodwell & Kumar, 2017) to measure patterns in plant hydraulic and stomatal controls: unique information (U_{VPD} and U_{SWP}) that only VPD or SWP provide about T ; synergistic information (S) that is provided only when both variables

are known together; and redundant information (R) that either variable can provide. We therefore evaluated the influence of both VPD and SWP on T which is otherwise challenging to disentangle with established parametric approaches (e.g., Novick et al., 2016).

Each model structure may produce the four types (U_{VPD} , U_{SWP} , S , and R) of information differently, and here we quantified model functional accuracy by comparing information flows in the models to those in the observations at the daily time scale following Bassiouni and Vico (2021). As such, we calculated five metrics as the relative difference between observed and modeled individual information partitioning components ($A_{f,U(VPD)}$, $A_{f,U(SWP)}$, $A_{f,S}$, $A_{f,R}$); and the sum of the absolute values of the partitioning accuracies ($A_{f,P} = |A_{f,U(SWP)}| + |A_{f,U(VPD)}| + |A_{f,S}| + |A_{f,R}|$). Additionally, we quantified predictive performance (A_p) in terms of the relative fraction of missing information about T in the model compared to observations. This metric is calculated as the difference between the entropy of observed T and the mutual information between observed and modeled T , normalized by the entropy of observed T . We estimated uncertainty by re-calculating the functional accuracy metrics from 10,000 bootstrapped samples of 80% of the data. For all accuracy metrics a value of 0 is a perfect match between models and observations. We note that VPD and SWP are correlated to different degrees at different time scales and thus the mutual information that VPD and SWP provide about T will quantify different relations at 30-min versus daily timesteps. In this study, we quantified predictive accuracy on a daily timestep since SWP is prescribed and thus the diurnal feedbacks between VPD, T and SWP are not represented in the modeling framework.

2.6.4. Structural Constraints on Information Flows

To isolate model structural constraints from parameterization errors, we generated a perturbed parameter ensemble and assessed the ability of alternate model parameterizations to accurately capture information flows. Parameters related to hydraulic and stomatal functioning were modified simultaneously within ranges defined by literature or expert solicitation (Table 2). An ensemble of 100 unique model parameterizations, sampled with a Latin-hypercube design, was generated using each model. We performed a Fourier amplitude sensitivity test (FAST; Saltelli & Bolado, 1998) to quantify the contribution of each parameter to the total variance in T . See Supporting Information S1 for further description (Text S2 in Supporting Information S1, Figures S3 and S4 in Supporting Information S1). We then calculated the information theory based performance metrics (Section 2.6.3) using the unique parameterizations of each model. If alternate parameterizations are unable to represent the flow of information from VPD and SWP to T accurately, we conclude that model structure is constraining performance.

3. Results

3.1. Diurnal Cycle of Ecosystem Processes

We examined simulated processes on hourly timescales to elucidate how model assumptions manifest in ecological functioning. For illustration, we show simulated days in mid-August 2010 when root-weighted soil water potential was below -1 MPa and daily maximum VPD increased from 1 to nearly 3 kPa (Figure 2). Generally, observed T peaked in the morning and tapered off throughout the day. All models adequately represented the diurnal transpiration except the Gain-Risk model which predicted T peaking in the afternoon. Similarly, observed G_c peaked in the morning and was reduced quickly throughout the day and all models simulated the shape of the diurnal cycle in G_c well. The Gain-Risk model simulates a slight increase in G_c in the afternoon due to the way G_c is calculated: the model determines the optimal transpiration rate from the Gain-Risk functions, and then stomatal conductance to water vapor, g_w , is calculated as $T = g_w * D_i$.

The simulated canopy water potential, P_c , illustrates the impact of the minimum ψ_l threshold set in the WUEi and WUE models. Once the threshold is reached the g_w is reduced to avoid cavitation and the minimum ψ_l is maintained throughout the day. Despite using more sophisticated hydraulic constraint functions, the Gain-Risk model simulates a similar diurnal shape in P_c . The hydraulic limitation in the BB-H and MED-H models modifies the g_1 parameter as a function of instantaneous ψ_l ; this implementation reduces GPP and T but there are no direct constraints on how low the canopy water potential can get and consequentially the mid-day canopy water potential reaches much lower values compared to the other models.

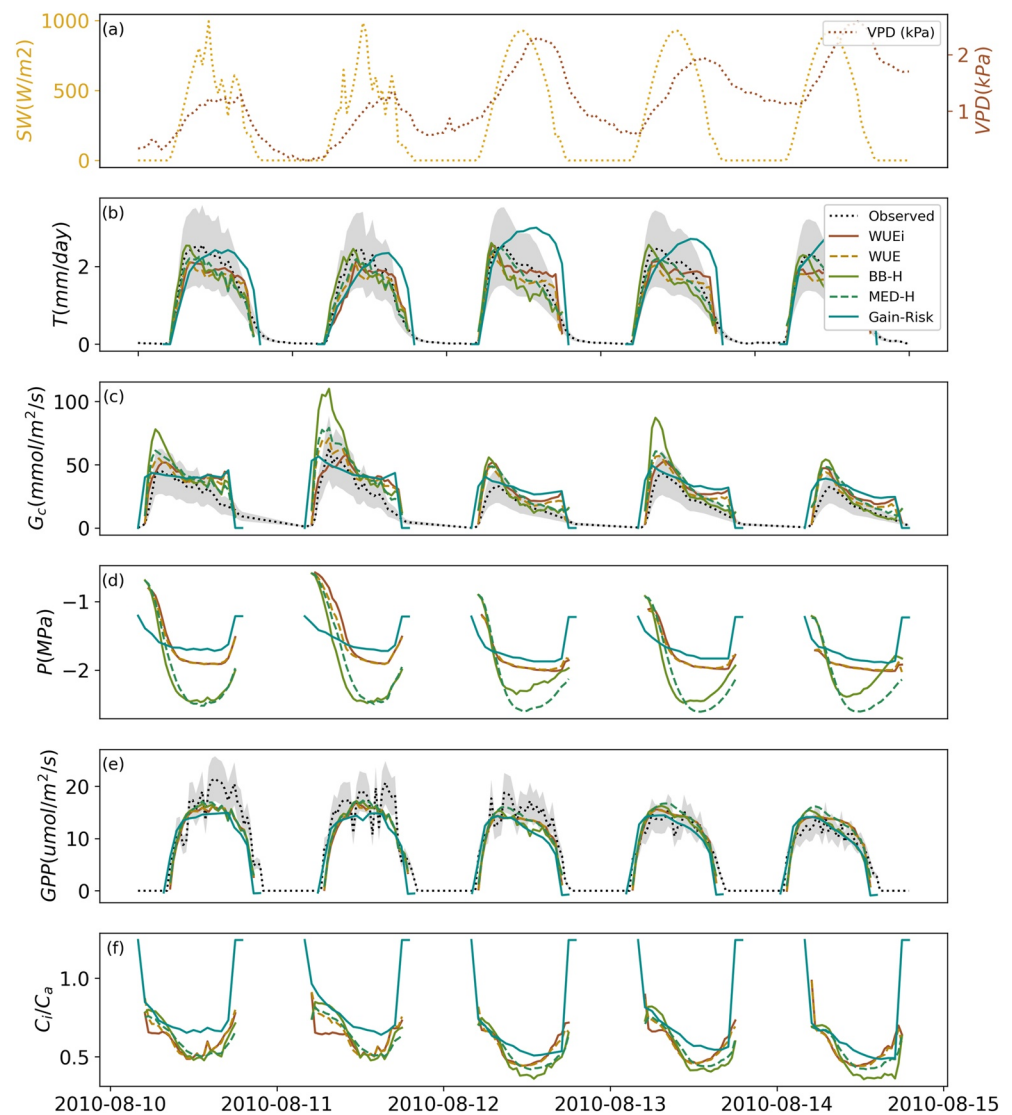


Figure 2. Diurnal cycle of measured or model simulated leaf level processes in mid-August 2010. (a) Incoming shortwave radiation (SW; W m^{-2}) and measured above-canopy vapor pressure deficit (VPD) (kPa), (b) transpiration (mm/day) with observations derived from sapflow measurements (black dotted lines), shading represents uncertainty of $\pm 40\%$ as per RUEHR et al. (2014), (c) canopy conductance ($\text{mmol m}^{-2} \text{leaf s}^{-1}$); observations estimated from sapflow measurements (black dotted lines) with shading representing uncertainty in sapflow estimates of transpiration, (d) simulated canopy water potential (MPa); (e) gross primary productivity ($\text{umol m}^{-2} \text{ground s}^{-1}$); and (f) simulated ratio of internal leaf CO_2 to atmospheric CO_2 concentrations. Root-weighted soil water potential remained nearly constant at -1 MPa during this period.

The magnitude and shape of gross primary productivity (GPP) is well captured by all models; however, the sub-daily variability is not well simulated. All models simulate a much smoother and consistent diurnal cycle of GPP whereas the observations are much more variable. The simulated ratio of intercellular CO_2 concentration to atmospheric CO_2 concentration (C_i/C_a) often reached minimum values around 0.5 by mid-afternoon.

All models adequately simulated the annual cycle of T and GPP for 2006–2018 (Figure S5 in Supporting Information S1) but to better understand model functional performance we evaluated model responses in varying environmental conditions. We assessed how models modify the shape of the diurnal cycle in T in response to VPD and SWP stress, according to four categories: high VPD and low SWP, high VPD and high SWP, low VPD and low SWP, and low VPD and high SWP (Figure 3). Low SWP is more negative and thus indicates higher drought stress. Generally, observed T peaks around 9 a.m. and stays relatively constant throughout the day, illustrating the conservative water use strategies typical of ponderosa pines. On days with high VPD there is a midday depression

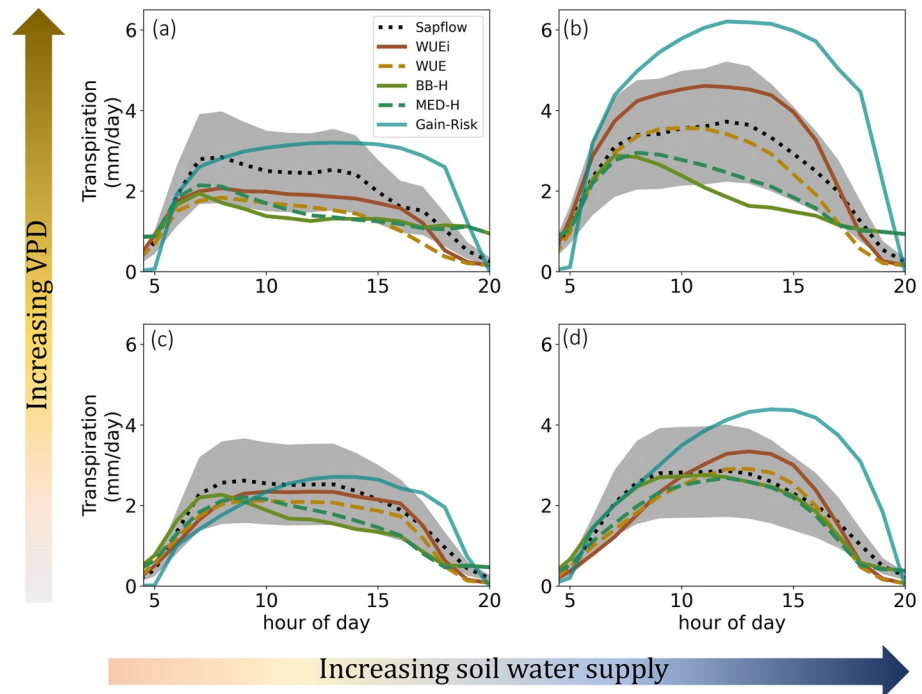


Figure 3. Average diurnal cycle of observed transpiration (black dashed) and modeled transpiration (colors) for days in July (2006–2018) with (a) maximum daily vapor pressure deficit (VPD) above 75th percentile and root-weighted soil water potential (SWP) below 25th percentile (18 days), (b) VPD > 75th percentile and SWP > 50th percentile (41 days) (c) VPD < 50th percentile and SWP < 25th percentile (28 days) and (d) VPD < 50th percentile and SWP > 50th percentile (119 days). Uncertainties in sapflow derived estimates of transpiration are estimated to be 40% (gray shading) as per Ruehr et al. (2014).

in T , but if soil moisture is not limiting transpiration resumes in the afternoon. All models alter the magnitude and shape of the simulated diurnal cycle in response to VPD and soil water potential, albeit to differing degrees. When soil water stress is high (Figures 3a and 3c) all models limit mid-day T and shift to more conservative water use. Models show this largest divergence from one another when VPD is high and soil water supply is also high (Figure 3b); high atmospheric demand increases the simulated T (relative to panel d) by varying amounts. Notably, in all categories the diurnal cycle simulated with the Gain-Risk model is markedly different from the observations and the other models. The Gain-Risk model simulates too much T when soil water supply is high (Figures 3b and 3d) and simulated T peaks in the late afternoon since the VPD constraint on T is applied indirectly via the carbon gain function.

3.2. Canopy Temperature Performance

In August when air temperatures typically peak at this site the observed T_{can} diverges from the T_{air} by mid-morning and can be two or three degrees warmer than T_{air} by mid-afternoon (Figure 4a). All models simulate an increase in T_{can} above T_{air} (<1°C) but fail to capture the large observed divergence of T_{can} from T_{air} . The damped response in modeled leaf temperature persists across models despite different representation of leaf temperature feedback mechanisms.

Prescribing observed leaf temperature in the MED-H model results in cooler morning leaf temperatures and warmer afternoon leaf temperatures (Figure 5a). The cooler morning leaf temperatures lead to more morning transpiration (Figure 5b). In August of 2015, the cumulative morning (8 a.m.–12 p.m.) transpiration was 9% higher when using the prescribed T_{can} . In the afternoons, the prescribed T_{can} was warmer than the modeled T_{can} , which resulted in lower transpiration rates. The cumulative afternoon (12–4 p.m.) transpiration in August 2015 was 4% lower when using the prescribed T_{can} . These results indicate that resolving biases in modeled T_{can} would lead to increased morning transpiration and decreased afternoon transpiration. These changes counteract one another, and the net effect was a 5% increase in total growing season (JJA) transpiration (not shown). Similarly,

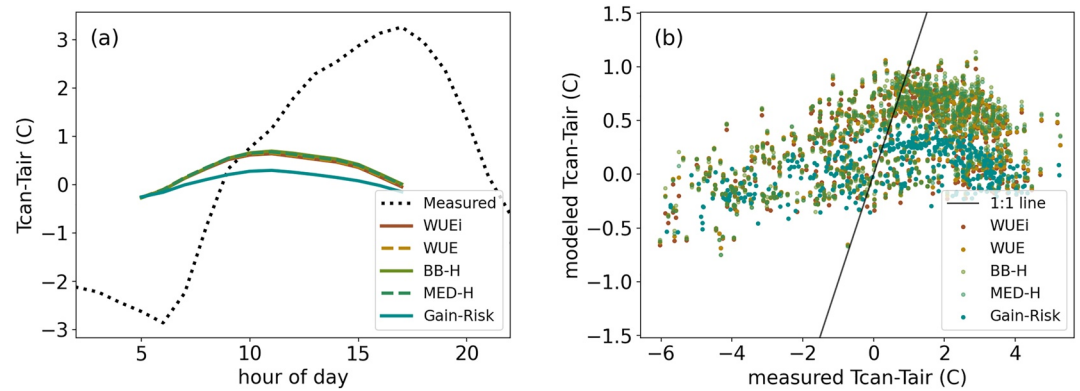


Figure 4. Measured and modeled canopy-air temperature in August 2015. (a) Average diurnal cycle and (b) measured versus modeled daytime mean canopy-air temperature. The temperature for the upper canopy layer is shown for the multi-layer soil-plant-atmosphere (SPA) model (leaf area weighted average of the sunlit and shaded fractions).

leaf water potentials were more negative in the mornings and less negative in the afternoons in the prescribed T_{can} simulations having the net effect of higher canopy water stress.

3.3. Sensitivity of Stomatal Conductance to VPD

When water stress was low (SWP above the 75th percentile) the observed G_c had a strong sensitivity to increasing VPD (Figure 6a). None of the models captured the sensitivity to VPD well, all models were less sensitive to VPD than observations. While models were generally indistinguishable, the WUEi model had the lowest sensitivity to VPD. This was expected given that the WUEi model optimizes $\Delta A/\Delta g_s$ and thus does not have a direct dependency on VPD. The WUE optimization has a direct dependency on VPD since stomatal efficiency is defined as $\Delta A/\Delta T$ and thus G_c is more sensitive to VPD as was shown by Bonan et al. (2014). The BB-H and MED-H models have similar sensitivities to VPD even though the MED-H model directly relates g_w to VPD whereas in BB-H g_w is a function of h . However, these results agree well with the findings of Franks et al. (2017) which illustrated that with equivalent parameterizations these two models have similar performance.

When water stress was high (SWP <25th percentile) the observed G_c was reduced and the sensitivity to VPD was weaker since G_c was already depressed (Figure 6b). The Gain-Risk model captured the magnitude of the depression in G_c when VPD was low, illustrating that soil water potential alone exhibits a strong constraint on G_c .

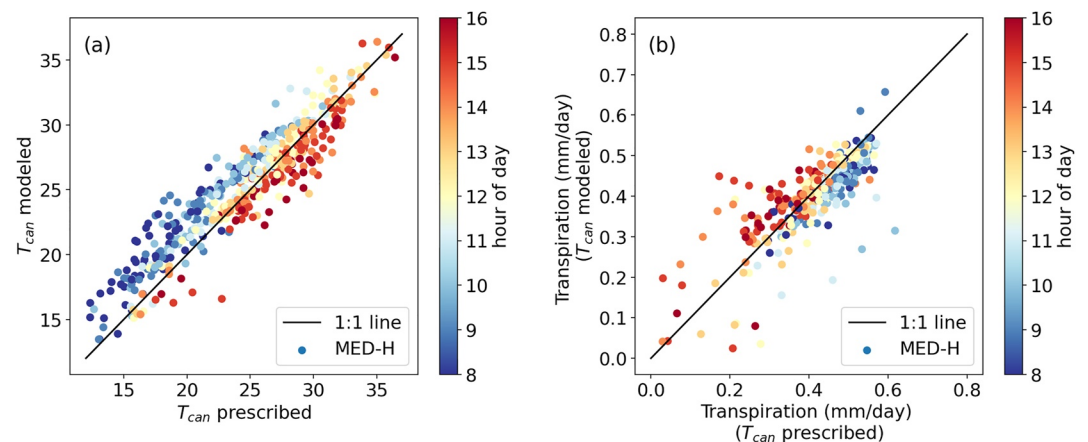


Figure 5. August 2015 canopy temperature (a) and transpiration (b) simulated with the MED-H model using the modeled canopy temperature (y-axis) or the prescribing the observed canopy temperature (x-axis). Shading represents the hour of day; data is shown on 30 min time intervals between 8 a.m. and 4 p.m.

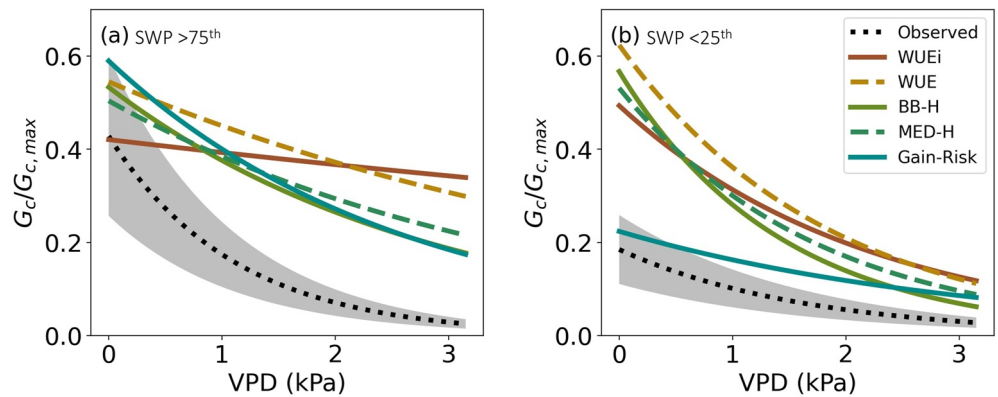


Figure 6. Observed (black) and modeled (color) sensitivity of canopy conductance ($G_c/G_{c,max}$) to vapor pressure deficit (VPD) when the soil water potential was greater than the 75th percentile (a), and when the soil water potential was less than the 25th percentile (b). Gray shading represents estimated error in G_c given 40% uncertainty in sapflow-derived transpiration.

in this model. The other models did not depress G_c sufficiently in response to water stress but were more sensitive to VPD, decreasing G_c quickly in response to higher VPD.

3.4. Water-Use Strategies

To compare water-use strategies resulting from each model, we examined how two measures of water use efficiency vary in response to plant water stress. We compared how models modify monthly mean daytime C_i/C_a and A/T in response to canopy water potential to differentiate among model responses to stress (Figure 7).

In the BB-H and MED-H models, C_i/C_a decreased linearly with canopy water potential. The Gain-Risk model also simulated a linear relationship, but C_i/C_a declined more rapidly with canopy water potential indicating that C_i was reduced more quickly under stress. The WUEi and WUE models do not allow canopy water potential to drop below a threshold (-2 MPa in this study) but the C_i/C_a can still be quite low when the minimum potential is reached, resulting in an asymptotic relationship. C_i/C_a is inversely related to the water-use efficiency, defined as A/T , and when canopy water potential was low all models simulated an increase in water-use efficiency (Figure 7b). The Gain-Risk model had the lowest water-use efficiency under unstressed conditions, likely due to the lack of constraints on T when the hydraulic risk is low. This is consistent with the overestimation of T during unstressed conditions seen in previous results. Models clearly simulate distinct relationships between these measures of water-use efficiency and canopy water potential during periods of both low and high environmental stress.

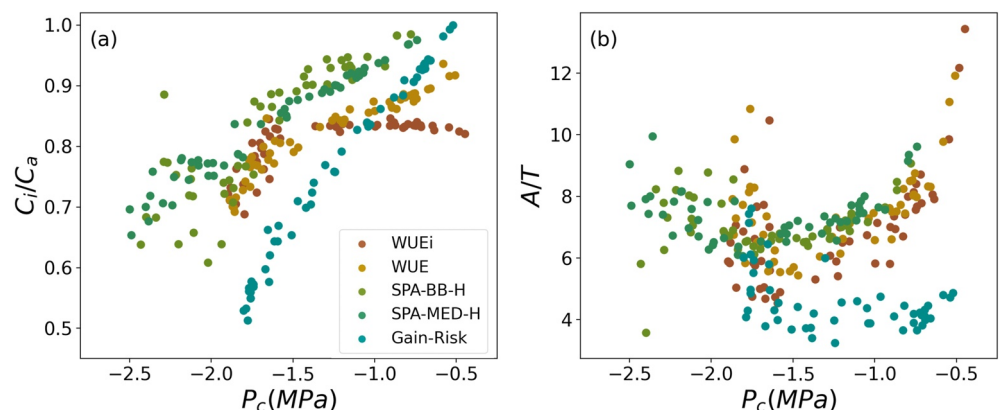


Figure 7. Simulated relationships between monthly mean daytime canopy water potential, P_c , and C_i/C_a (a) or assimilation/transpiration (A/T) (b) simulated for June, July, and August 2006–2018.

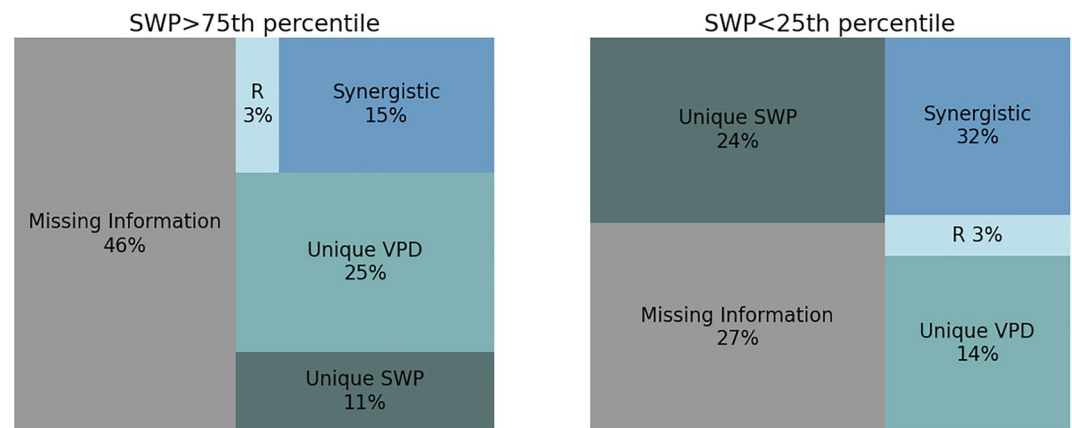


Figure 8. Reduction in uncertainty (mutual information) in daily transpiration rates attributable to vapor pressure deficit (VPD) and soil water potential (SWP), when SWP is above the 75th percentile (left) and below the 25th percentile (right). Mutual information is partitioned into synergistic, unique to VPD, unique to SWP, and redundant (R) information. The total area represents the entropy of transpiration and percentages are computed as the fraction of transpiration entropy. Missing information represents the fraction of transpiration entropy that is not shared with VPD and SWP.

3.5. Variability in Information Flows From VPD and SWP to T

The daily influence of VPD and SWP together on T was measured by their multi-variate mutual information partitioned into redundant, synergistic, and unique information components. When water stress was low (SWP > 75th percentile) the information from SWP and VPD together reduced 54% of uncertainty (entropy) in daily T (Figure 8). The remaining information about T can be attributed to the influence of the other environmental factors such as net radiation, which is a strong control on T in the spring when soil water is most available. The unique information from VPD reduced 25% of the uncertainty whereas the unique information from SWP and synergistic information reduced 11% and 15% of the uncertainty, respectively. This indicates that when water stress was low, VPD was a more influential control on T than SWP. When soil water stress was high (SWP < 25th percentile) the observed SWP and VPD reduced 73% of uncertainty in T (Figure 8). In the water-stressed late summer months, photosynthetically active radiation and temperature are usually less limiting and thus VPD and SWP are more influential on T compared to the early spring months. The unique information from SWP and VPD reduced 24% and 14% of the uncertainty, respectively, and the synergistic information reduced an additional 32%. In both the cases, the redundant information between VPD and SWP was small. Information partitioning for days between the 25th and 75th SWP percentiles are shown in Figure S6 in Supporting Information S1.

We evaluated how well each model represented the functional relationships among daily VPD, SWP and T by taking the difference between information flows calculated from measurements and calculated from model simulations. When soil water stress was high (SWP < 25th percentile) the more mechanistic models (WUEi, WUE, Gain-Risk) had higher predictive accuracy (lower $A_{f,p}$) than the semi-empirical models (BB-H, MED-H) and WUEi had the most accurate T estimates (Figure 9a). The WUE and MED-H models had overall higher functional accuracy ($A_{f,p}$ close to 0) (Figure 9b), despite not having the best predictive accuracy. The Gain-Risk model had the poorest partitioning accuracy (highest $A_{f,p}$), indicating that it may be reproducing the variability in T accurately but at the expense of poorer representation of the individual information flows. All models (excluding BB-H) accurately represented the unique information from SWP (Figure 9c) but the WUEi and Gain-Risk models overestimated the unique information from VPD (Figure 9d). The BB-H model overrepresented the synergistic information whereas the Gain-Risk model underestimated the synergistic information (Figure 9e). All models accurately captured the redundant information (Figure 9f).

Errors in functional accuracy could be attributable to multiple sources. First, there is uncertainty in transpiration derived from sapflow velocities which underestimate sap flux densities (Steppe et al., 2010) and scaling to the stand level requires accurate estimates of sapwood to ground area. Similarly, the soil water content is not measured at the soil-root interface but rather in bulk soil, thus the prescribed soil water potential does not capture the diurnal cycle in rhizosphere conductance. Second, by prescribing the soil water potential we do not allow transpiration during the day to reduce SWP near the roots, including feedbacks between transpiration and SWP would

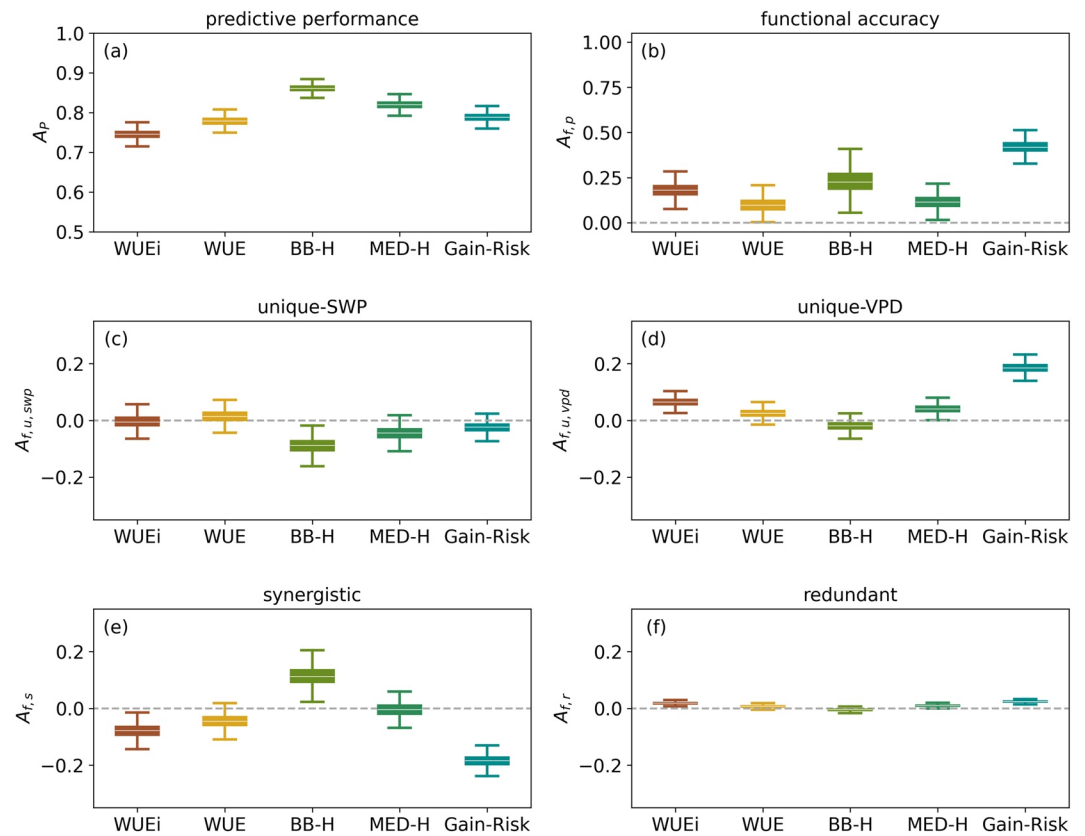


Figure 9. Performance evaluation of modeled daily transpiration (T) during the growing season (May–August) of 2006 through 2018 when soil water potential (SWP) was below the 25th percentile (high soil water stress). (a) Predictive accuracy (A_p , bits bit⁻¹) quantifies the relative fraction of information missing in the model about T compared to observations. (b) Functional accuracy ($A_{f,p} = |A_{f,U(SWP)}| + |A_{f,U(VPD)}| + |A_{f,S}| + |A_{f,R}|$, bits bit⁻¹) quantifies the relative difference between observed and modeled mutual information partitioning from SWP and VPD about T . The components of functional accuracy are partitioned into (c) unique from soil water potential ($A_{f,u,swp}$, bits bit⁻¹), (d) unique from VPD ($A_{f,u,vpd}$, bits bit⁻¹), (e) synergistic ($A_{f,s}$, bits bit⁻¹), and (f) redundant ($A_{f,r}$, bits bit⁻¹) information. Boxes represent the interquartile range of bootstrapped samples; whiskers represent 5th and 95th percentiles; and white lines represent medians. For all metrics a value of zero indicates a perfect model-data match.

likely amplify the modeled unique information from SWP and the synergistic information (discussed further in Section 4.4). Lastly, the model parameterizations were selected to be consistent across models, but alternate parameterizations may yield improved functional accuracy (see Section 3.6).

When water is not limiting (SWP > 75th percentile) the predictive performance of all models was indistinguishable (Figure S7 in Supporting Information S1). The BB-H had the best total functional accuracy (lowest $A_{f,p}$). The functional accuracy of the BB-H model outperformed all other models since all other models overestimate the unique information from VPD on T and underestimate the synergistic information from VPD and SWP.

3.6. Structural Constraints on Information Flows

To distinguish between model structural constraints and parameterization error we evaluated the functional accuracy of 100 unique parameterizations of each model. Model predictive accuracy was improved using alternate parameterizations of each model (Figure 10). However, no alternate model parameterization adequately represented the partitioning of mutual information from SWP and VPD about T ($A_{f,p}$), although there exist parameterizations that perform very well. All, or nearly all, parameterizations of each model underrepresented the unique information from soil water potential ($A_{f,U(SWP)}$), and overrepresented the unique information from VPD ($A_{f,U(VPD)}$), while parameterizations of each model accurately simulate the synergistic and redundant information. The underestimation of unique information from SWP in all model parameterizations indicates that our

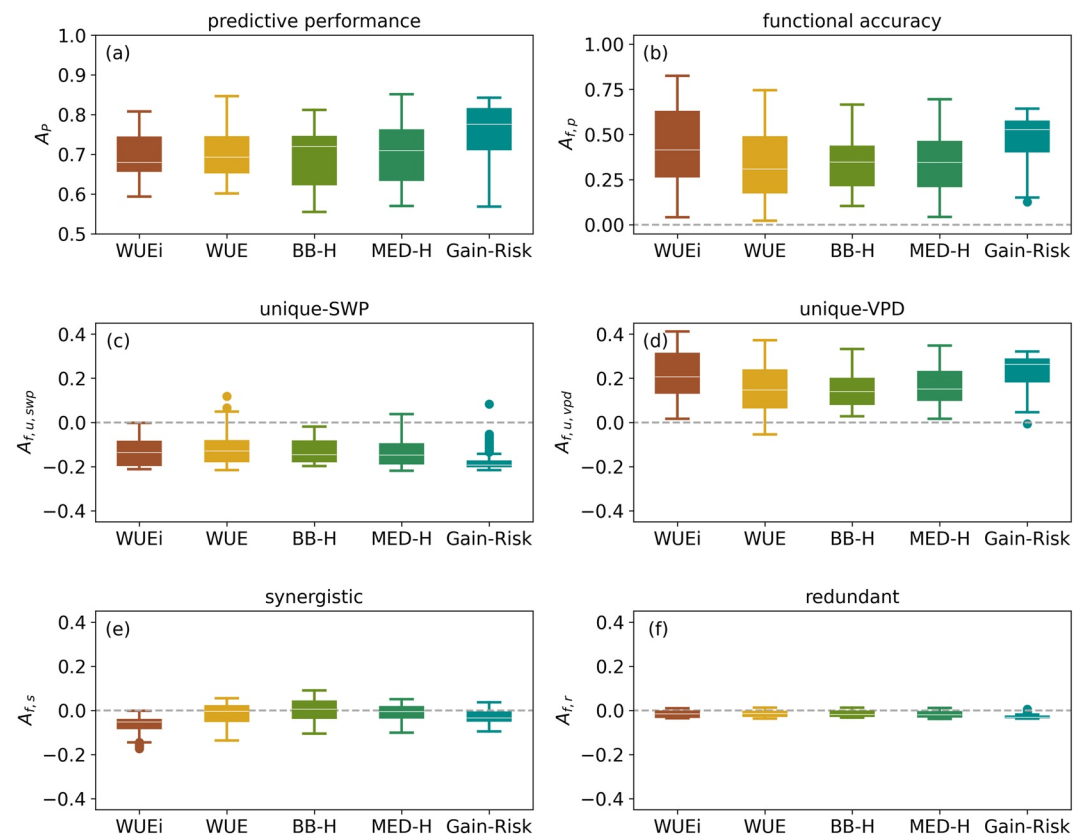


Figure 10. Same as Figure 9 but for 100 unique parameterizations of each model, and all days in May through August of 2006 and 2007 (i.e., not subset by soil water potential). Boxes represent the interquartile range of alternate model parameterizations; whiskers represent 5th and 95th percentiles; and white lines represent medians. For all metrics a value of zero indicates a perfect model-data match.

experimental design may be constraining important information flows. By prescribing SWP we limit feedbacks between transpiration and SWP but see Section 4.4.

Model parameterizations that have improved predictive accuracy generally also have improved functional accuracy (Figure S8 in Supporting Information S1). However, in the WUEi and BB-H models, the parameterizations with the best predictive accuracy (lowest A_p) achieve the improvement at the expense of some degree of functional accuracy (relatively higher $A_{f,p}$ values). This indicates that WUEi and BB-H are more likely to have compensating errors that result in improved predictive accuracy. Therefore, while there are common model structural deficiencies that may be attributable to the underlying experimental design (Figure 10), we can identify additional model structural errors for models with greater tradeoffs between predictive and functional accuracy (Figure S8 in Supporting Information S1).

This analysis highlights that alternate model parameterizations can yield similar performance across models, but it also indicates that structural constraints limit the model ability to represent information partitioning adequately. However, it is important to note that this was not an exhaustive parameter exploration, only parameters related to plant hydraulic and stomatal functioning were modified. It is likely that model predictive accuracy can be further improved by altering additional parameters, such as those related to soil properties or stand characteristics. Furthermore, our experimental design may constrain modeled information flows by prescribing SWP and removing sub-daily feedbacks between T and SWP.

4. Discussion

4.1. Representing Plant Hydraulic Strategies

Plant water and carbon relations are strongly tied to the ways plants respond to hydrologic stress. It's common to generalize plant hydraulic strategies along a continuum between isohydric and anisohydric behavior. Although this framework is over simplistic it can be useful (Kannenberget al., 2021) when comparing behavior with common environmental forcings. The hydraulic limitation imposed in this study in the BB-H and MED-H models represents more anisohydric behavior, as the model structure allows the canopy water potential to reach low mid-day levels (Figure 2). At low canopy water potentials, the BB-H and MED-H models increase the water-use efficiency (Figure 7) and constrain transpiration to peak in the morning (Figures 2 and 3).

Given the functional form of the hydraulic limitation we impose, alternate parameterizations cannot sufficiently represent the isohydric behavior characteristic of ponderosa pines. The BB-H and MED-H models originally used a fixed water-use efficiency, defined by the g_1 parameter. Here we implemented a hydraulic stress constraint which modifies the g_1 parameter in response to canopy water potential (Equation 6). The result is a linear reduction in C_i/C_a with reduced canopy water potential (Figure 7). A steeper hydraulic vulnerability constraint (achieved by modifying the b and c parameters in Equation 6) would prevent the canopy water potential from reaching very low values but only by modifying the g_1 parameter and thus reducing assimilation to near zero.

Kennedy et al. (2019) implemented a similar constraint in the CLM5 model but applied the hydraulic limitation by modifying V_{cmax} . Whether drought stress affects the water-use efficiency of plants or acts directly on photosynthetic capacity is still an open question. Zhou et al. (2013) found that downregulation of the g_1 parameter was insufficient to account for observed changes in GPP in response to water limitation, and thus modification of V_{cmax} was required. However, Lin et al. (2018) suggest that the g_1 parameter is not sensitive to water limitations and only the intercept, g_0 , and GPP are sensitive to soil water availability.

The structure of the WUEi and WUE models fundamentally represents isohydric water-use strategies (Fisher et al., 2006). The minimum leaf water potential threshold limits stomatal conductance at a prescribed canopy water potential which results in conservative water use. The WUEi and WUE models maintain relatively constant transpiration and canopy water potential throughout the day (Figure 2). The WUEi model also maintains near constant C_i/C_a until the minimum canopy water potential (-2 MPa) is reached (Figure 7). The stomatal efficiency parameter defines the marginal water cost of carbon that constrains the intrinsic water use efficiency ($\Delta A/\Delta g_s$) and thus the C_i/C_a . In the WUE model the stomatal efficiency parameter defines the instantaneous water use efficiency ($\Delta A/\Delta T$) and thus modifies the water use efficiency in response to VPD. Therefore, the decline in C_i/C_a with reduced canopy water potential simulated by the WUE model (Figure 7) is likely attributable to the correlation between VPD and canopy water potential.

Less conservative water-use behavior can be achieved by setting the minimum leaf water potential parameter to very low values (e.g., -6 MPa), then the stomatal efficiency parameter constrains plant water-use. However, there is a trade-off; the low settings of stomatal efficiency required to achieve anisohydric behavior also limit carbon assimilation. Williams et al. (1996) applied the WUEi model to a mixed deciduous broadleaf stand and was able to capture anisohydric behavior early in the growing season when canopy water potentials remained above the *minLWP* (set to -2.5 MPa) but in the late growing season when canopy water potentials were low the model constrained mid-day water-use and was unable to capture the observed anisohydric behavior.

The Gain-Risk model constrains the canopy water potential to avoid hydraulic damage. With the parameterization used in this application the model demonstrates conservative water use, maintaining relatively constant mid-day canopy water potentials (Figure 2). Because the Gain-Risk model varies the water-use efficiency optimally to maximize carbon gain while avoiding loss of hydraulic function, the model simulates the strongest reduction in monthly mean C_i/C_a in response to reduced canopy water potential (Figure 7). The Gain-Risk model can be parameterized to relax constraints on canopy water potential and can capture a range of water-use strategies as demonstrated by Sabot et al. (2020). However, the parameterization used here does not adequately capture the timing of water-use throughout the day (Figure 3). Ponderosa pines maximize canopy conductance and use water early in the day before the VPD gets too high (Figures 2 and 3), thus avoiding water loss while still maximizing carbon gain. The Gain-Risk model captures the early morning peak in canopy conductance (Figure 2), but it simulates transpiration peaking in the late afternoon, even under drought stress when the hydraulic risk is high. It

is possible that alternate plant trait combinations would alter the diurnal cycle of transpiration. In addition, transpiration in the Gain-Risk model is very sensitive to soil water potential (see Figure 6 in Venturas et al., 2018) and any error in the diurnal cycle of soil or rhizosphere water potential propagates to transpiration. Since our experimental design prescribed soil water potential, the absence of feedbacks between transpiration and rhizosphere water potential may be a major reason for the poor simulated diurnal canopy conductance patterns in this model (see Section 4.4). Future work is needed to determine if the Gain-Risk model can capture conservative water-use strategies on sub-daily temporal scales.

Emerging observational data streams have the potential to help advance our understanding the effects of drought stress on plant gas exchange. Near continuous measurements of leaf water potential are critical to provide information on how environmental conditions influence canopy water stress (Novick et al., 2022). While ground-based measurements are onerous to acquire, remotely sensed indicators of variability in plant water potential are emerging (Holtzman et al., 2021; Konings and Gentine, 2017) and may help elucidate large scale patterns in hydraulic functioning relevant for improving land surface model representation. Similarly, stable carbon isotopes provide information on plant water use efficiency (Condon et al., 1993; Farquhar & Richards, 1984; Farquhar et al., 1989) and the dynamics of isotopic discrimination can be used to evaluate how ecosystem models respond to environmental drivers on interannual timescales (Lavergne et al., 2019, Lavergne, Sandoval, et al., 2020a; Lavergne, Voelker, et al., 2020b). The National Ecological Observatory Network (NEON) measures atmospheric CO₂ isotope ratios across ecosystems at high temporal frequencies (Fiorella et al., 2021). We suggest that this observational network could serve as a valuable model testbed and encourage future cross-site model evaluation studies.

4.2. Canopy Temperature

Accurately modeling canopy temperatures is critical for representing ecological processes, particularly as heat waves become more frequent and severe under changing climate conditions. While the biophysical drivers of canopy temperature vary among ecosystems, canopy temperature is often more relevant to biological functioning than air temperature (Still et al., 2019). The observed canopy temperature diverged from air temperature by several degrees at this site. At night, canopy temperatures cooled below air temperatures and during the day canopy temperatures were nearly 3°C warmer than air temperatures (Figure 4). Similar behavior was shown by Kim et al. (2016) who found canopy temperature to be a strong predictor of net ecosystem exchange.

All models examined in this study were unable to capture the divergence of canopy temperature from air temperature (Figure 4). Other modeling studies have found similar model deficiencies, for example, Holm et al. (2014) found that the CLM4 was unable to reproduce the range of leaf temperatures observed at a tropical site. Duursma and Medlyn (2012) found that the MAESPA model was unable to capture the vertical profile of canopy temperatures using a multilayer canopy model. Venturas et al. (2018) compared leaf temperatures of Aspen measured with thermocouples to leaf temperatures simulated with the Gain-Risk model and found the model underestimated midday leaf temperatures (mean absolute leaf temperature error of 1.7°C or 5.2%). Biases in leaf temperature influence the calculation of leaf-to-air VPD (used in the calculation of transpiration) and can propagate through photosynthetic and stomatal optimization functions. Furthermore, since leaf metabolic processes depend non-linearly on leaf temperature small biases can manifest into large discrepancies, impacting model performance. When the observed leaf temperature was prescribed in the MED-H model, the cumulative growing season mean transpiration was 5% higher. The increased morning transpiration and decreased afternoon transpiration better matched the observed diurnal pattern of sapflow measurements (Figure 5).

These findings emphasize the need to address model deficiencies in the representation of canopy temperature. Big-leaf models have deficiencies in capturing canopy temperatures since the whole canopy experiences equivalent air temperatures. Although the multi-layer canopy model used in this study represents the vertical profile of radiation transfer and direct and diffuse radiation varies by canopy layer, the radiation scheme is not fully coupled to the leaf energy balance model. The SPA model assumes within-canopy air is well-mixed and thus applies the above canopy air temperature at all canopy layers. Other multilayer canopy models capture the vertical profiles of radiation and within-canopy air temperatures, which studies have found to improve simulated surface fluxes (Bonan et al., 2018; Chen et al., 2016). Bonan et al. (2021) demonstrated that using uniform vertical profiles of air temperatures in multilayer canopy models results in nearly identical fluxes as big-leaf models. When the well-mixed assumption is removed and the vertical profile of air temperatures are resolved, Bonan et al. (2021) showed considerable improvement in canopy fluxes. This suggests that a first step toward addressing canopy

temperature biases in multilayer models would be to resolve vertical air temperature profiles. A second step would be to examine the role of leaf boundary layer processes, which also likely contribute to leaf temperature biases. Finally, the heat capacity of the leaf can decrease when leaf water potentials are low which can amplify the leaf to air temperature gradient, but this process is not represented here.

4.3. Information Flows

We took an information theoretical approach to decompose multivariate mutual information between transpiration and its key drivers to assess process representation in models independently of parametric assumptions. Similarly to Bassiouni and Vico (2021), we found that all models had high overall functional accuracy (Figure 9). Generally, the more empirical models (BB-H & MED-H) had better functional accuracy when soil water was not limiting (Figure S6 in Supporting Information S1) while models with more mechanistic representations of hydraulic functioning (WUEi, WUE, Gain-Risk) had better functional accuracy when soil water availability was low (Figure 9). It is common for more empirical, multiplicative models (such as MED-H) to better represent synergistic information while more mechanistic additive models (such as Gain-Risk) can underestimate interactions among processes and thus trade synergistic for unique information. This result illustrates how semi-empirical models can compensate for incomplete process representation and capture functional relationships across scales, while incomplete processes in more mechanistic models are more easily discernible. The BB-H model had larger tradeoffs between predictive performance and functional accuracy compared to the Gain-Risk and MED-H models, pointing to the possibility that the BB-H model accurately estimated the variability in transpiration at the expense of poorer process representations (Figure S8 in Supporting Information S1). This finding was clearer from the information metrics than the individual process diagnostics.

Disentangling model structural constraints from parameterization error remains a significant challenge and new tools are needed to characterize sources of model uncertainty (e.g., Sexton et al., 2019). Here we illustrated how information theory based performance metrics can be combined with perturbed parameter ensembles to disaggregate uncertainty from model parameterization and model structure. We suggest that if no plausible alternative parameterization of a model can accurately partition the flow of information between transpiration and its key drivers, then there exists a structural constraint within the model (although observational data limitations and biases are also possible). For example, the underestimation of unique information from SWP may be due to the absence of non-stomatal hydraulic limitations on transpiration (Drake et al., 2017). Furthermore, the tradeoffs between model predictive and functional accuracy (Figure S8 in Supporting Information S1) can help illustrate when improved performance is achieved due to compensating errors. This approach can be leveraged to advance model development by identifying model processes that need further examination.

This study builds upon the work of Bassiouni and Vico (2021) by implementing stomatal models within multi-layer canopy (and big-leaf) ecosystem models and solving optimization routines numerically. The findings of both studies agree; more mechanistic representations of plant hydraulic functioning did not substantially improve predictive or functional accuracy, although other studies have found contrasting results (e.g., Eller et al., 2020; Sabot et al., 2020, 2022). Our results indicate that hydraulic-modified semi-empirical models, in particular MED-H, can be effectively adapted to incorporate hydraulic constraints based on measurable plant traits. Model evaluation metrics based on information flows allowed us to go beyond evaluating model performance based on magnitude and seasonality (e.g., Sabot et al., 2020) and examine the causal relationships among the physiological controls on transpiration. The performance metrics also complement the analysis of individual model sensitivities of G_c to VPD and C_i/C_a to P_c because they help differentiate between effective functional differences and predictive accuracy. However, additional analyses are needed to further interpret the mechanisms driving information-based performance metrics and test whether models with improved functional accuracy perform better under non-stationary climate conditions, as well as incorporating transpiration-soil water potential feedbacks and how those may influence canopy conductance dynamics. We encourage cross-scale model evaluations spanning a range of ecosystems and advocate for the use of information theory to evaluate causal relationships in complex ecological systems.

4.4. Caveats of Prescribing Soil Water Potential

In our experimental setup we opted to prescribe the SWP to ensure fairer comparisons among models. This decision was made for two reasons, first, the SPA and Gain-Risk models use different soil water retention functions, thus even with prescribed soil water content the soil water potential would vary between models, particularly when soil moisture is low. Second, if a model has a high transpiration bias in the spring the soil moisture might be lower than the other models by the end of summer, confounding direct comparisons among models. While this design constrains potential confounding effects, it also has limitations. Our soil water content measurements do not represent the soil-root interface and thus there is little diurnal cycle in soil water potential. By prescribing SWP we explicitly do not allow transpiration during the day to reduce SWP near the roots, but this feedback is likely influential on stomatal closure. The rhizosphere is a key interface controlling how plants respond to drought; studies have shown that the loss of soil hydraulic conductivity is a driver of stomatal closure (Carminati & Javaux, 2020). The Gain-Risk model explicitly represents the rhizosphere conductance and the feedback between transpiration and rhizosphere water potential influences stomatal function. The diurnal variation in rhizosphere conductance is an important feedback in the Gain-Risk model (and in reality) and constraining this value may be an important source of the error in how the model regulates stomatal conductance throughout the day. Further research is needed to assess the role of feedbacks between root and soil hydraulic conductivity on model representation of stomatal functioning.

5. Conclusions

As the consequences of model representation of stomatal functioning become apparent at large scales (e.g., Kala et al., 2016), much effort has gone into updating the representation of hydraulic functioning in Earth System Models (e.g., Eller et al., 2020; Kennedy et al., 2019; Sabot et al., 2020; Sabot et al., 2022). To ensure processes are adequately captured across scales, model evaluations must go beyond mean state and variability of leaf-level gas exchange measurements and find new ways to diagnose functional performance and leverage new analytical techniques. Here, we compared a suite of ecosystem models with different representations of hydraulic constraints on stomatal function and identified model specific strengths and deficiencies at a semi-arid ponderosa pine site. We found that models generally performed similarly under unstressed conditions, but performance diverged under atmospheric and soil drought. The more empirical models over estimated synergistic information flows between soil water potential and vapor pressure deficit to transpiration, while the more mechanistic models were overly deterministic.

This analysis highlights three directions for future ecosystem model development and evaluation: First, additional exploration of parameter space is needed to determine if model structure constrains the flexibility of models to represent a broad spectrum of (an)isohydric behavior. Second, models were unable to capture the magnitude of the divergence of canopy temperature from air temperature and given the crucial role of canopy temperature in simulating metabolic processes, diagnosing the causes of model biases should be a priority. Lastly, information theoretic approaches hold promise as a valuable tool to help characterize ecosystem function and elucidate differences attributable to model structure but future work is needed to parse parameter uncertainty from model structural uncertainty.

Data Availability Statement

Model code, configuration, and simulations, observational data, and PYTHON scripts required to reproduce this analysis are openly available at <https://doi.org/10.5281/zenodo.7145415>.

References

- Anderegg, W. R. L., Wolf, A., Arango-Velez, A., Choat, B., Chmura, D. J., Jansen, S., et al. (2018). Woody plants optimise stomatal behaviour relative to hydraulic risk. *Ecology Letters*, *21*(7), 968–977. <https://doi.org/10.1111/ele.12962>
- Aphalo, P. J., & Jarvis, P. G. (1991). Do stomata respond to relative humidity? *Plant, Cell and Environment*, *14*(1), 127–132. <https://doi.org/10.1111/j.1365-3040.1991.tb01379.x>
- Ball, J. T., Woodrow, I. E., & Berry, J. A. (1987). A model predicting stomatal conductance and its contribution to the control of photosynthesis under different environmental conditions. In J. Biggins (Ed.), *Progress in Photosynthesis Research: Volume 4 Proceedings of the VIIth International Congress on Photosynthesis Providence, Rhode Island, USA, 10–15, 1986* (pp. 221–224). Springer Netherlands. https://doi.org/10.1007/978-94-017-0519-6_48

Acknowledgments

The authors would like to thank Matt Williams and Luke Smallman for technical support for the SPA model, and Henry Todd for technical support with the Gain-Risk model. This work was funded by the National Science Foundation, Division of Environmental Biology, through the macrosystems biology and NEON-enable science program Grant DEB-1802885. MB received funding from the European Commission and Swedish Research Council for Sustainable Development (FORMAS) (Grant 2018-02787) in the frame of the international consortium iAquaduct financed under the 2018 Joint call of the Water-Works2017 ERA-NET Cofund. MDV was supported by H2020-MSCA-IF-2019 Grant 882216.

- Bassiouni, M., & Vico, G. (2021). Parsimony vs predictive and functional performance of three stomatal optimization principles in a big-leaf framework. *New Phytologist*, 231(2), 586–600. <https://doi.org/10.1111/nph.17392>
- Bonan, G. B. (1995). Land-atmosphere CO₂ exchange simulated by a land surface process model coupled to an atmospheric general circulation model. *Journal of Geophysical Research*, 100(D2), 2817–2831. <https://doi.org/10.1029/94JD02961>
- Bonan, G. B., Patton, E. G., Finnigan, J. J., Baldocchi, D. D., & Harman, I. N. (2021). Moving beyond the incorrect but useful paradigm: Reevaluating big-leaf and multilayer plant canopies to model biosphere-atmosphere fluxes—A review. *Agricultural and Forest Meteorology*, 306, 108435. <https://doi.org/10.1016/j.agrformet.2021.108435>
- Bonan, G. B., Patton, E. G., Harman, I. N., Oleson, K. W., Finnigan, J. J., Lu, Y., & Burakowski, E. A. (2018). Modeling canopy-induced turbulence in the Earth system: A unified parameterization of turbulent exchange within plant canopies and the roughness sublayer (CLM-ml v0). *Geoscientific Model Development*, 11(4), 1467–1496. <https://doi.org/10.5194/gmd-11-1467-2018>
- Bonan, G. B., Williams, M., Fisher, R. A., & Oleson, K. W. (2014). Modeling stomatal conductance in the Earth system: Linking leaf water-use efficiency and water transport along the soil–plant–atmosphere continuum. *Geoscientific Model Development*, 7(5), 2193–2222. <https://doi.org/10.5194/gmd-7-2193-2014>
- Buckley, T. N. (2005). The control of stomata by water balance. *New Phytologist*, 168(2), 275–292. <https://doi.org/10.1111/j.1469-8137.2005.01543.x>
- Buckley, T. N. (2017). Modeling stomatal conductance. *Plant Physiology*, 174(2), 572–582. <https://doi.org/10.1104/pp.16.01772>
- Buckley, T. N. (2019). How do stomata respond to water status? *New Phytologist*, 224(1), 21–36. <https://doi.org/10.1111/nph.15899>
- Carminati, A., & Javaux, M. (2020). Soil rather than xylem vulnerability controls stomatal response to drought. *Trends in Plant Science*, 25(9), 868–880. <https://doi.org/10.1016/j.tplants.2020.04.003>
- Chen, Y., Ryder, J., Bastrikov, V., McGrath, M. J., Naudts, K., Otto, J., et al. (2016). Evaluating the performance of land surface model ORCHIDEE-CAN v1.0 on water and energy flux estimation with a single- and multi-layer energy budget scheme. *Geoscientific Model Development*, 9(9), 2951–2972. <https://doi.org/10.5194/gmd-9-2951-2016>
- Condon, A. G., Richards, R. A., & Farquhar, G. D. (1993). Relationships between carbon isotope discrimination, water use efficiency and transpiration efficiency for dryland wheat. *Australian Journal of Agricultural Research*, 44(8), 1693–1711. <https://doi.org/10.1071/ar9931693>
- Cover, T. M., & Thomas, J. A. (2012). *Elements of information theory*. John Wiley & Sons.
- Cowan, I. (1986). *Economics of carbon fixation in higher plants. On the economy of plant form and function*. In T. J. Givnish (Ed.), (pp. 133–170). Cambridge University Press.
- Cowan, I. R., & Farquhar, G. D. (1977). *Stomatal function in relation to leaf metabolism and environment. Integration of activity in the higher plant* (pp. 471–505). Cambridge University Press. Retrieved from <https://pubmed.ncbi.nlm.nih.gov/756635/>
- Cox, P. M., Huntingford, C., & Harding, R. J. (1998). A canopy conductance and photosynthesis model for use in a GCM land surface scheme. *Journal of Hydrology*, 212(213), 79–94. [https://doi.org/10.1016/S0022-1694\(98\)00203-0](https://doi.org/10.1016/S0022-1694(98)00203-0)
- Damour, G., Simonneau, T., Cochard, H., & Urban, L. (2010). An overview of models of stomatal conductance at the leaf level. *Plant, Cell and Environment*, 33(9), 1419–1438. <https://doi.org/10.1111/j.1365-3040.2010.02181.x>
- Drake, J. E., Power, S. A., Duursma, R. A., Medlyn, B. E., Aspinwall, M. J., Choat, B., et al. (2017). Stomatal and non-stomatal limitations of photosynthesis for four tree species under drought: A comparison of model formulations. *Agricultural and Forest Meteorology*, 247, 454–466. <https://doi.org/10.1016/j.agrformet.2017.08.026>
- Duursma, R. A., & Medlyn, B. E. (2012). MAESPA: A model to study interactions between water limitation, environmental drivers and vegetation function at tree and stand levels, with an example application to [CO₂] × drought interactions. *Geoscientific Model Development*, 5(4), 919–940. <https://doi.org/10.5194/gmd-5-919-2012>
- Eller, C. B., Rowland, L., Mencuccini, M., Rosas, T., Williams, K., Harper, A., et al. (2020). Stomatal optimization based on xylem hydraulics (SOX) improves land surface model simulation of vegetation responses to climate. *New Phytologist*, 226(6), 1622–1637. <https://doi.org/10.1111/nph.16419>
- Farquhar, G. D., Ehleringer, J. R., & Hubick, K. T. (1989). Carbon isotope discrimination and photosynthesis. *Annual Review of Plant Physiology and Plant Molecular Biology*, 40(1), 503–537. <https://doi.org/10.1146/annurev.pp.40.060189.002443>
- Farquhar, G. D., & Richards, R. A. (1984). Isotopic composition of plant carbon correlates with water-use efficiency of wheat genotypes. *Functional Plant Biology*, 11(6), 539–552. <https://doi.org/10.1071/pp9840539>
- Farquhar, G. D., & von Caemmerer, S. (1982). Modelling of photosynthetic response to environmental conditions. In O. L. Lange, P. S. Nobel, C. B. Osmond, & H. Ziegler (Eds.), *Physiological plant ecology II: Water relations and carbon assimilation* (pp. 549–587). Springer. https://doi.org/10.1007/978-3-642-68150-9_17
- Farquhar, G. D., von Caemmerer, S., & Berry, J. A. (1980). A biochemical model of photosynthetic CO₂ assimilation in leaves of C₃ species. *Planta*, 149(1), 78–90. <https://doi.org/10.1007/bf00386231>
- Feng, X. (1999). Trends in intrinsic water-use efficiency of natural trees for the past 100–200 years: A response to atmospheric CO₂ concentration. *Geochimica et Cosmochimica Acta*, 63(13–14), 1891–1903. [https://doi.org/10.1016/s0016-7037\(99\)00088-5](https://doi.org/10.1016/s0016-7037(99)00088-5)
- Fiorella, R. P., Good, S. P., Allen, S. T., Guo, J. S., Still, C. J., Noone, D. C., et al. (2021). Calibration strategies for detecting macroscale patterns in NEON atmospheric carbon isotope observations. *Journal of Geophysical Research: Biogeosciences*, 126(3), e2020JG005862. <https://doi.org/10.1029/2020JG005862>
- Fisher, R. A., Williams, M., Do Vale, R. L., Da Costa, A. L., & Meir, P. (2006). Evidence from Amazonian forests is consistent with isohydric control of leaf water potential. *Plant, Cell and Environment*, 29(2), 151–165. <https://doi.org/10.1111/j.1365-3040.2005.01407.x>
- Franks, P. J., Berry, J. A., Lombardozzi, D. L., & Bonan, G. B. (2017). Stomatal function across temporal and spatial scales: Deep-time trends, land-atmosphere coupling and global models. *Plant Physiology*, 174(2), 583–602. <https://doi.org/10.1104/pp.17.00287>
- Goodwell, A. E., & Bassiouni, M. (2022). Source relationships and model structures determine information flow paths in ecohydrologic models. *Water Resources Research*, 58(9), e2021WR031164. <https://doi.org/10.1029/2021WR031164>
- Goodwell, A. E., Jiang, P., Ruddell, B. L., & Kumar, P. (2020). Debates—Does information theory provide a new paradigm for Earth science? Causality, interaction, and feedback. *Water Resources Research*, 56(2), e2019WR024940. <https://doi.org/10.1029/2019WR024940>
- Goodwell, A. E., & Kumar, P. (2017). Temporal information partitioning: Characterizing synergy, uniqueness, and redundancy in interacting environmental variables. *Water Resources Research*, 53(7), 5920–5942. <https://doi.org/10.1002/2016WR020216>
- Grossiord, C., Buckley, T. N., Cernusak, L. A., Novick, K. A., Poulter, B., Siegwolf, R. T. W., et al. (2020). Plant responses to rising vapor pressure deficit. *New Phytologist*, 226(6), 1550–1566. <https://doi.org/10.1111/nph.16485>
- Hill, T. C., Williams, M., & Moncrieff, J. B. (2008). Modeling feedbacks between a boreal forest and the planetary boundary layer. *Journal of Geophysical Research*, 113(D15), D15122. <https://doi.org/10.1029/2007JD009412>
- Holm, J. A., Jardine, K., Guenther, A. B., Chambers, J. Q., & Tribuzy, E. (2014). Evaluation of MEGAN-CLM parameter sensitivity to predictions of isoprene emissions from an Amazonian rainforest. *Atmospheric Chemistry and Physics Discussions*, 14(17), 23995–24041. <https://doi.org/10.5194/acpd-14-23995-2014>

- Holtzman, N. M., Anderegg, L. D. L., Kraatz, S., Mavrovic, A., Sonnentag, O., Pappas, C., et al. (2021). L-band vegetation optical depth as an indicator of plant water potential in a temperate deciduous forest stand. *Biogeosciences*, *18*(2), 739–753. <https://doi.org/10.5194/bg-18-739-2021>
- Irvine, J., Law, B. E., Kurpius, M. R., Anthoni, P. M., Moore, D., & Schwarz, P. A. (2004). Age-related changes in ecosystem structure and function and effects on water and carbon exchange in ponderosa pine. *Tree Physiology*, *24*(7), 753–763. <https://doi.org/10.1093/treephys/24.7.753>
- Irvine, J., Law, B. E., Martin, J. G., & Vickers, D. (2008). Interannual variation in soil CO₂ efflux and the response of root respiration to climate and canopy gas exchange in mature ponderosa pine. *Global Change Biology*, *14*(12), 2848–2859. <https://doi.org/10.1111/j.1365-2486.2008.01682.x>
- Johnson, D. M., Woodruff, D. R., McCulloh, K. A., & Meinzer, F. C. (2009). Leaf hydraulic conductance, measured in situ, declines and recovers daily: Leaf hydraulics, water potential and stomatal conductance in four temperate and three tropical tree species. *Tree Physiology*, *29*(7), 879–887. <https://doi.org/10.1093/treephys/tpp031>
- Kala, J., De Kauwe, M. G., Pitman, A. J., Medlyn, B. E., Wang, Y.-P., Lorenz, R., & Perkins-Kirkpatrick, S. E. (2016). Impact of the representation of stomatal conductance on model projections of heatwave intensity. *Scientific Reports*, *6*(1), 23418. <https://doi.org/10.1038/srep23418>
- Kannenbergh, S. A., Guo, J. S., Novick, K. A., Anderegg, W. R. L., Feng, X., Kennedy, D., et al. (2021). Opportunities, challenges and pitfalls in characterizing plant water-use strategies. *Functional Ecology*, *36*(1), 13945–37. <https://doi.org/10.1111/1365-2435>
- Kennedy, D., Swenson, S., Oleson, K. W., Lawrence, D. M., da Fisher, R., Costa, A. C. L., & Gentine, P. (2019). Implementing plant hydraulics in the community land model, version 5. *Journal of Advances in Modeling Earth Systems*, *11*(2), 485–513. <https://doi.org/10.1029/2018MS001500>
- Kim, Y., Still, C. J., Hanson, C. V., Kwon, H., Greer, B. T., & Law, B. E. (2016). Canopy skin temperature variations in relation to climate, soil temperature, and carbon flux at a ponderosa pine forest in Central Oregon. *Agricultural and Forest Meteorology*, *226–227*, 161–173. <https://doi.org/10.1016/j.agrformet.2016.06.001>
- Konings, A. G., & Gentine, P. (2017). Global variations in ecosystem-scale isohydricity. *Global Change Biology*, *23*(2), 891–905. <https://doi.org/10.1111/gcb.13389>
- Kwon, H., Law, B. E., Thomas, C. K., & Johnson, B. G. (2018). The influence of hydrological variability on inherent water use efficiency in forests of contrasting composition, age, and precipitation regimes in the Pacific Northwest. *Agricultural and Forest Meteorology*, *249*(15), 488–500. <https://doi.org/10.1016/j.agrformet.2017.08.006>
- Lavergne, A., Graven, H., De Kauwe, M. G., Keenan, T. F., Medlyn, B. E., & Prentice, I. C. (2019). Observed and modelled historical trends in the water-use efficiency of plants and ecosystems. *Global Change Biology*, *25*(7), 2242–2257. <https://doi.org/10.1111/gcb.14634>
- Lavergne, A., Sandoval, D., Hare, V. J., Graven, H., & Prentice, I. C. (2020a). Impacts of soil water stress on the acclimated stomatal limitation of photosynthesis: Insights from stable carbon isotope data. *Global Change Biology*, *26*(12), 7158–7172. <https://doi.org/10.1111/gcb.15364>
- Lavergne, A., Voelker, S., Csank, A., Graven, H., de Boer, H. J., Daux, V., et al. (2020b). Historical changes in the stomatal limitation of photosynthesis: Empirical support for an optimality principle. *New Phytologist*, *225*(6), 2484–2497. <https://doi.org/10.1111/nph.16314>
- Law, B. E., Cescatti, A., & Baldocchi, D. D. (2001). Leaf area distribution and radiative transfer in open-canopy forests: Implications for mass and energy exchange. *Tree Physiology*, *21*(12–13), 777–787. <https://doi.org/10.1093/treephys/21.12-13.777>
- Li, B., & Good, S. P. (2021). Information-based uncertainty decomposition in dual-channel microwave remote sensing of soil moisture. *Hydrology and Earth System Sciences*, *25*(9), 5029–5045. <https://doi.org/10.5194/hess-25-5029-2021>
- Lin, C., Gentine, P., Huang, Y., Guan, K., Kimm, H., & Zhou, S. (2018). Diel ecosystem conductance response to vapor pressure deficit is suboptimal and independent of soil moisture. *Agricultural and Forest Meteorology*, *250–251*, 24–34. <https://doi.org/10.1016/j.agrformet.2017.12.078>
- Lin, Y.-S., Medlyn, B. E., Duursma, R. A., Prentice, I. C., Wang, H., Baig, S., et al. (2015). Optimal stomatal behaviour around the world. *Nature Climate Change*, *5*(5), 459–464. <https://doi.org/10.1038/nclimate2550>
- Mäkelä, A., Berninger, F., & Hari, P. (1996). Optimal control of gas exchange during drought: Theoretical analysis. *Annals of Botany*, *77*(5), 461–468. <https://doi.org/10.1006/anbo.1996.0056>
- Manzoni, S., Vico, G., Palmroth, S., Porporato, A., & Katul, G. (2013). Optimization of stomatal conductance for maximum carbon gain under dynamic soil moisture. *Advances in Water Resources*, *62*, 90–105. <https://doi.org/10.1016/j.advwatres.2013.09.020>
- Medlyn, B. E., Duursma, R. A., Eamus, D., Ellsworth, D. S., Prentice, I. C., Barton, C. V. M., et al. (2011). Reconciling the optimal and empirical approaches to modelling stomatal conductance. *Global Change Biology*, *17*(6), 2134–2144. <https://doi.org/10.1111/j.1365-2486.2010.02375.x>
- Meinzer, F. C., Johnson, D. M., Lachenbruch, B., McCulloh, K. A., & Woodruff, D. R. (2009). Xylem hydraulic safety margins in woody plants: Coordination of stomatal control of xylem tension with hydraulic capacitance. *Functional Ecology*, *23*(5), 922–930. <https://doi.org/10.1111/j.1365-2435.2009.01577.x>
- Mencuccini, M., Manzoni, S., & Christoffersen, B. (2019). Modelling water fluxes in plants: From tissues to biosphere. *New Phytologist*, *222*(3), 1207–1222. <https://doi.org/10.1111/nph.15681>
- Misson, L., Panek, J. A., & Goldstein, A. H. (2004). A comparison of three approaches to modeling leaf gas exchange in annually drought-stressed ponderosa pine forests. *Tree Physiology*, *24*(5), 529–541. <https://doi.org/10.1093/treephys/24.5.529>
- Monteith, J., & Unsworth, M. (1990). *Principles of environmental physics: Plants, animals, and the atmosphere*. Academic Press.
- Novick, K. A., Ficklin, D. L., Baldocchi, D., Davis, K. J., Ghezzehei, T. A., Konings, A. G., et al. (2022). Confronting the water potential information gap. *Nature Geoscience*, *15*(3), 158–164. <https://doi.org/10.1038/s41561-022-00909-2>
- Novick, K. A., Ficklin, D. L., Stoy, P. C., Williams, C. A., Bohrer, G., Oishi, A. C., et al. (2016). The increasing importance of atmospheric demand for ecosystem water and carbon fluxes. *Nature Climate Change*, *6*(11), 1023–1027. <https://doi.org/10.1038/nclimate3114>
- Reinhardt, E., Scott, J., Gray, K., & Keane, R. (2006). Estimating canopy fuel characteristics in five conifer stands in the Western United States using tree and stand measurements. *Canadian Journal of Forest Research*, *36*(11), 2803–2814. <https://doi.org/10.1139/x06-157>
- Ruddell, B. L., Drewry, D. T., & Nearing, G. S. (2019). Information theory for model diagnostics: Structural error is indicated by trade-off between functional and predictive performance. *Water Resources Research*, *55*(8), 6534–6554. <https://doi.org/10.1029/2018WR023692>
- Ruddell, B. L., & Kumar, P. (2009). Ecohydrologic process networks: 1. Identification. *Water Resources Research*, *45*(3). <https://doi.org/10.1029/2008WR007279>
- Ruehr, N. K., Law, B. E., Quandt, D., & Williams, M. (2014). Effects of heat and drought on carbon and water dynamics in a regenerating semi-arid pine forest: A combined experimental and modeling approach. *Biogeosciences*, *11*(15), 4139–4156. <https://doi.org/10.5194/bg-11-4139-2014>
- Sabot, M. E. B., De Kauwe, M. G., Pitman, A. J., Medlyn, B. E., Ellsworth, D. S., Martin-StPaul, N. K., et al. (2022). One stomatal model to rule them all? Toward improved representation of carbon and water exchange in global models. *Journal of Advances in Modeling Earth Systems*, *14*(4), e2021MS002761. <https://doi.org/10.1029/2021MS002761>
- Sabot, M. E. B., De Kauwe, M. G., Pitman, A. J., Medlyn, B. E., Verhoef, A., Ukkola, A. M., & Abramowitz, G. (2020). Plant profit maximization improves predictions of European forest responses to drought. *New Phytologist*, *226*(6), 1638–1655. <https://doi.org/10.1111/nph.16376>
- Saltelli, A., & Bolado, R. (1998). An alternative way to compute Fourier amplitude sensitivity test (FAST). *Computational Statistics & Data Analysis*, *26*(4), 445–460. [https://doi.org/10.1016/S0167-9473\(97\)00043-1](https://doi.org/10.1016/S0167-9473(97)00043-1)

- Schwarz, P. A., Law, B. E., Williams, M., Irvine, J., Kurpius, M., & Moore, D. (2004). Climatic versus biotic constraints on carbon and water fluxes in seasonally drought-affected ponderosa pine ecosystems. *Global Biogeochemical Cycles*, 18(4). <https://doi.org/10.1029/2004GB002234>
- Sexton, D. M. H., Karmalkar, A. V., Murphy, J. M., Williams, K. D., Boutle, I. A., Morcrette, C. J., et al. (2019). Finding plausible and diverse variants of a climate model. Part 1: Establishing the relationship between errors at weather and climate time scales. *Climate Dynamics*, 53(1), 989–1022. <https://doi.org/10.1007/s00382-019-04625-3>
- Shannon, C. E. (1948). A mathematical theory of communication. *The Bell System Technical Journal*, 27(3), 379–423. <https://doi.org/10.1002/j.1538-7305.1948.tb01338.x>
- Smallman, T. L., Moncrieff, J. B., & Williams, M. (2013). WRFv3.2-SPAv2: Development and validation of a coupled ecosystem–atmosphere model, scaling from surface fluxes of CO₂ and energy to atmospheric profiles. *Geoscientific Model Development*, 6(4), 1079–1093. <https://doi.org/10.5194/gmd-6-1079-2013>
- Sperry, J. S., & Love, D. M. (2015). What plant hydraulics can tell us about responses to climate-change droughts. *New Phytologist*, 207(1), 14–27. <https://doi.org/10.1111/nph.13354>
- Sperry, J. S., Venturas, M. D., Anderegg, W. R. L., Mencuccini, M., Mackay, D. S., Wang, Y., & Love, D. M. (2017). Predicting stomatal responses to the environment from the optimization of photosynthetic gain and hydraulic cost. *Plant, Cell and Environment*, 40(6), 816–830. <https://doi.org/10.1111/pce.12852>
- Sperry, J. S., Venturas, M. D., Todd, H. N., Trugman, A. T., Anderegg, W. R. L., Wang, Y., & Tai, X. (2019). The impact of rising CO₂ and acclimation on the response of US forests to global warming. *Proceedings of the National Academy of Sciences*, 116(51), 25734–25744. <https://doi.org/10.1073/pnas.1913072116>
- Sperry, J. S., Wang, Y., Wolfe, B. T., Mackay, D. S., Anderegg, W. R. L., McDowell, N. G., & Pockman, W. T. (2016). Pragmatic hydraulic theory predicts stomatal responses to climatic water deficits. *New Phytologist*, 212(3), 577–589. <https://doi.org/10.1111/nph.14059>
- Steppe, K., De Pauw, D. J. W., Doody, T. M., & Teskey, R. O. (2010). A comparison of sap flux density using thermal dissipation, heat pulse velocity and heat field deformation methods. *Agricultural and Forest Meteorology*, 150(7), 1046–1056. <https://doi.org/10.1016/j.agrformet.2010.04.004>
- Still, C., Powell, R., Aubrecht, D., Kim, Y., Helliker, B., Roberts, D., et al. (2019). Thermal imaging in plant and ecosystem ecology: Applications and challenges. *Ecosphere*, 10(6), e02768. <https://doi.org/10.1002/ecs2.2768>
- Sus, O., Poyatos, R., Barba, J., Carvalhais, N., Llorens, P., Williams, M., & Vilalta, J. M. (2014). Time variable hydraulic parameters improve the performance of a mechanistic stand transpiration model. A case study of Mediterranean Scots pine sap flow data assimilation. *Agricultural and Forest Meteorology*, 198–199, 168–180. <https://doi.org/10.1016/j.agrformet.2014.08.009>
- Thomas, C. K., Law, B. E., Irvine, J., Martin, J. G., Pettijohn, J. C., & Davis, K. J. (2009). Seasonal hydrology explains interannual and seasonal variation in carbon and water exchange in a semiarid mature ponderosa pine forest in central Oregon. *Journal of Geophysical Research*, 114(G4), G04006. <https://doi.org/10.1029/2009JG001010>
- Tuzet, A., Perrier, A., & Leuning, R. (2003). A coupled model of stomatal conductance, photosynthesis and transpiration. *Plant, Cell and Environment*, 26(7), 1097–1116. <https://doi.org/10.1046/j.1365-3040.2003.01035.x>
- Venturas, M. D., Sperry, J. S., Love, D. M., Frehner, E. H., Allred, M. G., Wang, Y., & Anderegg, W. R. L. (2018). A stomatal control model based on optimization of carbon gain versus hydraulic risk predicts aspen sapling responses to drought. *New Phytologist*, 220(3), 836–850. <https://doi.org/10.1111/nph.15333>
- Venturas, M. D., Todd, H. N., Trugman, A. T., & Anderegg, W. R. L. (2021). Understanding and predicting forest mortality in the Western United States using long-term forest inventory data and modeled hydraulic damage. *New Phytologist*, 230(5), 1896–1910. <https://doi.org/10.1111/nph.17043>
- Wang, Y., Sperry, J. S., Anderegg, W. R. L., Venturas, M. D., & Trugman, A. T. (2020). A theoretical and empirical assessment of stomatal optimization modeling. *New Phytologist*, 227(2), 311–325. <https://doi.org/10.1111/nph.16572>
- Williams, M., Law, B. E., Anthoni, P. M., & Unsworth, M. H. (2001a). Use of a simulation model and ecosystem flux data to examine carbon-water interactions in ponderosa pine. *Tree Physiology*, 21(5), 287–298. <https://doi.org/10.1093/treephys/21.5.287>
- Williams, M., Rastetter, E. B., Fernandes, D. N., Goulden, M. L., Wofsy, S. C., Shaver, G. R., et al. (1996). Modelling the soil-plant-atmosphere continuum in a Quercus-Acer stand at Harvard Forest: The regulation of stomatal conductance by light, nitrogen and soil/plant hydraulic properties. *Plant, Cell and Environment*, 19(8), 911–927. <https://doi.org/10.1111/j.1365-3040.1996.tb00456.x>
- Williams, M., Rastetter, E. B., Shaver, G. R., Hobbie, J. E., Carpino, E., & Kwiatkowski, B. L. (2001b). Primary production of an arctic watershed: An uncertainty analysis. *Ecological Applications*, 11(6), 1800–1816. [https://doi.org/10.1890/1051-0761\(2001\)011\[1800:PPOAAW\]2.0.CO;2](https://doi.org/10.1890/1051-0761(2001)011[1800:PPOAAW]2.0.CO;2)
- Williams, M., Schwarz, P. A., Law, B. E., Irvine, J., & Kurpius, M. R. (2005). An improved analysis of forest carbon dynamics using data assimilation. *Global Change Biology*, 11(1), 89–105. <https://doi.org/10.1111/j.1365-2486.2004.00891.x>
- Wolf, A., Anderegg, W. R., & Pacala, S. W. (2016). Optimal stomatal behavior with competition for water and risk of hydraulic impairment. *Proceedings of the National Academy of Sciences*, 113(46), E7222–E7230. <https://doi.org/10.1073/pnas.1615144113>
- Xu, X., Medvigy, D., Powers, J. S., Becknell, J. M., & Guan, K. (2016). Diversity in plant hydraulic traits explains seasonal and inter-annual variations of vegetation dynamics in seasonally dry tropical forests. *New Phytologist*, 212(1), 80–95. <https://doi.org/10.1111/nph.14009>
- Yang, J., Duursma, R. A., De Kauwe, M. G., Kumarathunge, D., Jiang, M., Mahmud, K., et al. (2019). Incorporating non-stomatal limitation improves the performance of leaf and canopy models at high vapour pressure deficit. *Tree Physiology*, 39(12), 1961–1974. <https://doi.org/10.1093/treephys/tpz103>
- Zhou, S., Duursma, R. A., Medlyn, B. E., Kelly, J. W. G., & Prentice, I. C. (2013). How should we model plant responses to drought? An analysis of stomatal and non-stomatal responses to water stress. *Agricultural and Forest Meteorology*, 182–183, 204–214. <https://doi.org/10.1016/j.agrformet.2013.05.009>

References From the Supporting Information

- Domec, J.-C., Warren, J. M., Meinzer, F. C., Brooks, J. R., & Coulombe, R. (2004). Native root xylem embolism and stomatal closure in stands of Douglas-fir and ponderosa pine: Mitigation by hydraulic redistribution. *Oecologia*, 141(1), 7–16. <https://doi.org/10.1007/s00442-004-1621-4>
- Koepke, D. F., & Kolb, T. E. (2013). Species variation in water relations and xylem vulnerability to cavitation at a forest-woodland Ecotone. *Forest Science*, 59(5), 524–535. <https://doi.org/10.5849/forsci.12-053>
- Love, D. M., Venturas, M. D., Sperry, J. S., Brooks, P. D., Pettit, J. L., Wang, Y., et al. (2019). Dependence of aspen stands on a subsurface water subsidy: Implications for climate change impacts. *Water Resources Research*, 55(3), 1833–1848. <https://doi.org/10.1029/2018WR023468>

- McKay, M. D., Beckman, R. J., & Conover, W. J. (1979). A comparison of three methods for selecting values of input variables in the analysis of output from a computer code. *Technometrics*, *21*(2), 239–245. <https://doi.org/10.2307/1268522>
- Saxton, K. E., Rawls, W. J., Romberger, J. S., & Papendick, R. I. (1986). Estimating generalized soil-water characteristics from texture. *Soil Science Society of America Journal*, *50*(4), 1031–1036. <https://doi.org/10.2136/sssaj1986.03615995005000040039x>
- Stout, D. H., & Sala, A. (2003). Xylem vulnerability to cavitation in *Pseudotsuga menziesii* and *Pinus ponderosa* from contrasting habitats. *Tree Physiology*, *23*(1), 43–50. <https://doi.org/10.1093/TREEPHYS/23.1.43>